

DAMMSÄKERHET

Seepage Monitoring by Resistivity and Streaming Potential Measurements at Hällby Embankment Dam 1996-1999

Rapport 00:15

Seepage Monitoring by Resistivity and Streaming Potential Measurements at Hällby Embankment Dam 1996-1999

Elforsk rapport 00:15

Seepage Monitoring by Resistivity and Streaming Potential Measurements at Hällby Embankment Dam 1996-1999

Elforsk rapport 00:15

Sam Johansson and Johan Friborg HydroResearch Sam Johansson AB Torleif Dahlin Dept. of Geotechnology, Lund University

Sammanfattning

Kontinuerlig mätning av resistiviteten startade 1996 på Hällbydammen med syfte att undersöka om metoden kan användas för att bestämma vattenströmningen genom dammen. Mätningar har pågått sedan hösten 1996, med endast smärre driftsavbrott. Denna rapport omfattar mätningar till och med oktober 1999.

Mätning görs längs dammen i tre mätsektioner: under vattenytan på uppströmssidan, på dammkrönet samt på nerströmssidan. Resultatet har visat att en säsongsvariation föreligger, vilken delvis beror på vattenströmningens storlek. Påverkan sker dessutom av fukthalts- och temperaturvariationer vid markytan. De senare medför tjälning av marken som i sin tur medför mättekniska svårigheter.

De mätningar som sker på uppströmssidan under vatten uppvisar bäst mätkvalitet. Dessvärre kan endast viss utvärdering ske eftersom elektrodernas läge måste fastställas innan ytterligare utvärdering kan ske.

Mätningarna i övriga mätsektioner har en förhållandevis hög brusnivå varför resultatet måste bearbetas innan analys. Detta har gjorts genom medianfiltrering på 15 dagars basis, varvid erforderlig noggrannhet har uppnåtts höger nerströmssida. För de återstående mätsektionerna, höger och vänster dammkrön har önskad mätkvalitet ej kunnat erhållas. Dock är data från vänster dammkrön av tillräcklig kvalitet för att kunna användas vid försök till flödesutvärdering. Såväl mät- som utvärderingsteknik har förbättrats jämfört med föregående utvärderingar. Ytterligare förbättringar har också framkommit, speciellt beträffande installation och utvärderingsmetodik.

Med utgångspunkt från resistivitetsmätningarna har flödet i dammen kunnat utvärderas till ca 10⁻⁶ m³/s,m². Zoner med avvikande egenskaper och/eller variationer förekommer, men är troligtvis av mindre betydelse.

Mätning av strömningspotentialen (SP) har utförts med samma mätsystem och samma elektroder som använts för resistivitetsmätningarna. Dessa elektroder är ej ideala för SP-mätningar, där icke polariserbara elektroder bör användas. Mätningarna visar stabila värden både beträffande den strömningsinducerade potentialen samt den effekt som uppkommer genom polariseringen av elektroden. De mätningar som gjorts på land uppvisar en säsongsvariation, förmodligen orsakad av förändringar (temperatur, fukt etc) kring elektroden. Mätresultatet i undervattenselektroderna uppvisar mindre variationer. Några förändringar av vattenströmningen har ej kunnat observeras.

Den mätnings- och utvärderingsteknik som nu använts visar att resistivitets och SP-mätningar kan användas för att få en bättre bild av vattenströmingen genom dammen. Fortfarande återstår arbete innan ett system för automatisk mätning och utvärdering kan presenteras. Potential för ett sådant system finns, vilket framgått av inledande mätningar på Sädvadammen. Där installerades 1999 ett system baserat på erfarenheterna från Hällby. Mätningarna i Sädva visar att mätkvaliteten kan förbättras avsevärt, vilket också medför förbättrade utvärderingsmöjligheter.

Summary

A system for continuous resistivity monitoring was installed in Hällby embankment dam in 1996. The result from three years measurements shows a seasonal resistivity variation in the dam. This depends on the seepage flow, which influences the resistivity due to the seasonal variation in temperature and concentration of total dissolved solids in the reservoir. However, freezing, soil moisture and electrical disturbances also affect the resistivity data.

Measured data using land-based electrodes at Hällby is associated with unsatisfactory noise levels, whereas the underwater electrodes provide good to excellent data quality. To achieve the data quality that is needed, it is essential to ascertain a better electrode grounding, as achieved for the new installation at the Sädva dam. It should also be possible to develop techniques for better installation of electrodes in the upper part of the core using a drilling device as well. Electrode installation at larger depths inside the dam core, may also be possible to improve the resolution at depth, that probably will be mandatory for application on higher dams.

The processing and interpretation methodology of time series of resistivity data is still at a relatively early stage. Significant improvements in for example noise handling for the data are envisaged in the future. Time-lapse inversion appears to be a powerful way to stabilise the inversion process, and the results are more consistent than in previous data processing. However, a more systematic assessment of the potential and limitations need to be carried out, against field data as well as numerical models.

The seepage flow was evaluated from seasonal variation in the resistivity data using methods similar to those employed for seepage evaluation from temperature data. Seepage flow in the order of 10^{-6} m³/s,m² was achieved. The result implies that resistivity monitoring can provide measurements of time-dependent processes such as internal erosion. The seasonal resistivity variation also implies that resistivity measurement at a single time in a dam must be interpreted carefully as the result is incomplete without the time variation.

SP-data recorded at Hällby using stainless steel electrodes are stable and repeatable. Although the data are apparently contaminated with a polarization component, this component is also stable, and to a certain extent possible to remove or account for. However, even after attempting to remove the polarization component, evidence of seepage variation are week and inconclusive. Seasonal variation occur only in the land-based profiles, indicating that there is no real variation in the streaming potentials, rather the variation is caused by changes in the local electrode environment.

Overall results and experience do not yet allow an installation of an automatic monitoring and evaluation system. However, both monitoring and evaluation methods can be improved and such a system seems to be possible to achieve in the future. The method may then be an alternative for seepage monitoring in existing dams, without seepage monitoring systems, or where conventional seepage monitoring is complicated.

Content

1	IN	NTRODUCTION	1
2	P	ARAMETERS AND MONITORING PRINCIPLES	2
	2.1		
		STREAMING POTENTIAL	
3	M	IONITORING INSTALLATIONS AT HÄLLBY	7
	3.1	THE EMBANKMENT DAM	
	3.2	Installations	
	3.3	MONITORING PROGRAM	
	3.4	DATA PROCESSING AND PRESENTATION	
		DATA QUALITY ASSESSMENT	
4	R	ESULTS FROM RESISTIVITY MEASUREMENTS AT HÄLLBY DAM	14
	4.1	GENERAL EXPERIENCE	
	4.2	RESERVOIR	
	4.3	LEFT DAM CREST	
	4.4	RIGHT DAM CREST	
	4.5	DOWNSTREAM RIGHT DAM	
	4.6	UPSTREAM LEFT AND RIGHT DAM	26
5	R	ESULTS FROM SP MONITORING AT HÄLLBY	28
	5.1	General	28
	5.2	LEFT DAM	28
	5.3	RIGHT DAM	31
	5.4	SUMMARY AND SYNTHESIS	33
6	T	EMPORAL RESISTIVITY VARIATION AND SEEPAGE EVALUATION	35
	6.1	General	35
	6.2	LEFT DAM CREST	35
		RIGHT DAM DOWNSTREAM	
	6.4	DISCUSSION	41
7	D	DISCUSSION AND CONCLUSIONS	43
8	Α	CKNOWLEDGEMENTS	46
9	R	EFERENCES	47

1 Introduction

Monitoring of the collected drainage water from embankment dams is the normal way of seepage monitoring in dams. This gives the total seepage flow over the entire dam or within a limited section. The potential to detect local internal erosion is however limited. Seepage monitoring systems with higher accuracy and resolution are therefore needed. Of particular importance are methods that are able to register small changes in the seepage rate through a dam, and thus detect internal erosion at an early stage before it starts to affect the safety of the dam.

Internal erosion is a major cause of failures in embankment dams. The seepage flow increases slowly, closely coupled to the induced material transport that can take place over a long time. Research and development of geophysical methods to detect seepage changes and internal erosion started in Sweden in the late 80ties with temperature measurements (Johansson, 1991).

Based on the development of automated resistivity surveying made by Dahlin (1993), a new concept for seepage monitoring in embankment dams was presented. This new concept was based on seasonal temperature and resistivity variations. Initial tests were made in two dams, Lövön and Moforsen, between 1993 and 1995 (Johansson and Dahlin 1996). Based on these first results a permanent installation for resistivity monitoring was made at Hällby embankment dam in 1996. Since the monitoring system allowed to also measure streaming potential (SP), it was decided to collect SP-data. Based on the experience from Hällby dam a new installation was made at Sädva dam 1999. The first long term SP-measurements started however at the Sourva dam in 1993 (Triumf and Thunehed, 1996).

This report is summarizes result and experiences from the first three years of measurement. The main objectives are to:

- Present long term data of resistivity and SP;
- Evaluate all data with the same and improved methodology; and
- Establish a picture of the seepage pattern through the dam and foundation.

2 Parameters and monitoring principles

2.1 Resistivity

2.1.1 General

It is well known that the resistivity in soils depends on material properties, such as clay content, porosity and saturation. This is the fundamental base for soil investigations with resistivity measurements (see for example Ward 1990 and Parasnis 1986). However, resistivity also depends on pore water properties, such as the concentration of total dissolved solids (TDS) and temperature. The latter is normally neglected in resistivity measurements, but it cannot be ignored in the case of resistivity measurements in embankment dams.

2.1.2 Monitoring in embankment dams

This application of resistivity monitoring is based on the experience from temperature measurements in embankment dams. Seasonal temperature variations in the dams have been detected due to the seasonal temperature variation in the reservoir and the seepage water flow. Since the resistivity in the dam depends partly on the temperature it will also exhibit seasonal variations. The resistivity depends furthermore on the TDS in the water and this too varies seasonally. The combination of these parameters, temperature and TDS, is expressed by the resistivity of the reservoir water, which will create a seasonal variation in the resistivity in the dam due to the seepage through the dam.

Embankment dams with normal dam performance have material properties that are essentially constant over long periods of time. In such cases the resistivity variation is a function of seepage alone. If internal erosion occurs, however, it also affects the material properties due to increased porosity and loss of fines. Unfortunately, an increasing porosity decreases the resistivity while a loss of fines increases it, and this makes seepage evaluation more difficult.

Regular resistivity measurements in two embankment dams (Lövön and Moforsen) started in 1993, after model calculations had indicated that seasonal resistivity variation could be detected using resistivity measurements. The objectives of this pilot research project were to measure the resistivity variations in the dams and, if possible, to quantify the seepage from the measured resistivities. The aim was primarily to extend the methodology developed for the evaluation of temperature measurements to the evaluation of resistivity measurements, rather than to develop a complete description of the transport theory. The project was reported by Johansson and Dahlin (1996). Based on these experiences a monitoring system was installed in 1996 at the embankment dam at Hällby power plant.

2.1.3 Basic concepts and assumptions

Solute transport within a dam is an advective process related to the seepage flow. The seepage flow is coupled to the temperature field, which is formed as a result of advective flow and heat conduction. It is necessary therefore to consider a set of coupled transport processes for heat and solute. Heat conduction, mainly through the unsaturated parts of a dam, may also be important for low seepage flow rates and small dams. Geothermal flow may be important for large dams.

The seasonal variation of the absolute resistivity in the reservoir water is separated into two parts when the seepage water, q, passes through the dam, see Figure 1.

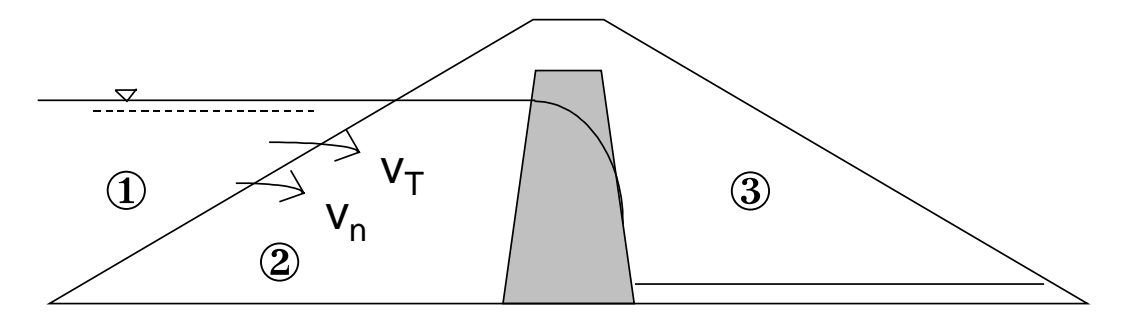


Figure 1 Basic transport processes in an embankment dam.

- 1. Seasonal variation of TDS and temperature
- 2. Advective transport with seepage and heat conduction
- 3. Heat exchange with the air

v_T - Thermal velocity

v_n - Pore velocity

The solutes penetrate into the dam with the pore velocity v_n (= q/θ , where θ is the porosity) while the temperature travels with the thermal velocity v_T (= qC_w/C , where C_w is the volumetric heat capacity in the water and C in the soil). The resistivity variation in the dam is therefore a combined result of these two transport processes.

2.1.4 Seepage evaluation methods

The quantitative interpretation of water flow through the dam is based on the fact that a variation in resistivity in the reservoir water will propagate into the dam with the seepage water. The variation due to variations in TDS will travel with the pore velocity, whereas the variation due to temperature will move with the thermal velocity as described above.

The simplest method of seepage evaluation consists of comparing extreme values for the absolute resistivity in the reservoir and the interpreted resistivity in the embankment dam. This is the lagtime method. This method is one-dimensional and neglects both heat loss and dispersion effects. It requires the lagtime t_d and the length of the seepage pathway x as input data, that gives the transport velocity ($=x/t_d$). The assumptions concerning heat transport are not valid for small leakage zones where the heat losses

around the leakage zone can be large. The approximations are more valid for larger zones, with cross sections of some 10 m² or more. This size corresponds to the cell size used for inversion of the resistivity data.

If the temperature is constant at the boundary the seepage flow only depends on the TDS transport, and this travels with the pore velocity. The evaluated seepage flow from these assumptions q_{TDS} will thus be a function of the porosity:

$$q_{TDS} = \frac{\theta x}{t_d}$$
 Eq. (1)

On the other hand, if the TDS in the reservoir is constant it is the temperature changes that cause the main resistivity variation in the dam. Seepage evaluation can then be performed with the lagtime method developed for temperature measurements, based on the thermal velocity. The evaluated seepage flow q_T depends on the volumetric heat capacity in the soil (C_0) and is:

$$q_T = \frac{C_0 x}{C_w t_d}$$
 Eq. (2)

These two estimated values of the seepage flow (q_{TDS}) and q_T can be interpreted as limits for the real seepage flow q since it can be proved that the pore velocity is larger than the thermal velocity. However, these limits do not include the entire range of uncertainty values. It is in many cases difficult to estimate the length of the real seepage pathway as well as the lagtime. The dispersion will not influence the lagtime, but it strongly affects the temporal variations of the resistivity and complicates the evaluation of the lagtime. However, in the absence of more accurate methods, such limits may sometimes be good enough to estimate the seepage flow in dams.

The seepage flow limit depends on the dam height, and the value of about $10^{-6} \text{m}^3/\text{s,m}^2$ is valid for typical Swedish dams with a height of about 30 meters. Zones where seepage changes occur, or zones with anomalous leakage, can therefore be located in such dams with a detection level of about $10^{-6} \text{m}^3/\text{s,m}^2$.

2.2 Streaming potential

2.2.1 Background

Streaming potentials constitute one of several sources of self-potentials, i.e. spontaneous electrical potential variations in the ground. Other examples of self-potential sources are mineralisations and thermal activity. For investigation of seepage through embankment dams, streaming potentials are especially interesting since they have a direct primary coupling to the flow of ground water. Other self-potential sources are rarely important in dams, and if present they would generally be considered as a source of noise. Metal

installations in the dam, like bare cables or fences, could act as such noise sources as they produce self-potentials of the mineralisation type.

2.2.2 Creation of streaming potentials

In general, all mineral surfaces in contact with an electrolyte will develop an electric charge. To preserve electro-neutrality, this surface charge must be balanced by an equal amount of opposite charges distributed in the electrolyte. The charges in the electrolyte constitute the electrical double layer, which will contain an excess of charges compared to the bulk of the electrolyte. When there is a flow of electrolyte past the mineral surface part of the double layer is sheared off, and some of the excess charges move downstream with the fluid flow. This charge separation is the basic physical mechanism behind streaming potentials. For most geological materials, the surface charge is negative and consequently areas of ground water influx become negatively charged, whereas areas of outflow acquire a positive charge.

Although not strictly true it may be illuminating to view the creation of streaming potential anomalies as a step-wise process:

- 1. A groundwater flow pattern is established. Hydraulic boundary conditions and the distribution of hydraulic conductivity in the subsurface determine this.
- 2. The water flow shears off part of the electrical double layer creating a convection current density, which causes a separation of charge.
- 3. The charge separation sets up an electric field, which will drive an electric current through the ground. The distribution of the current depends on the position of the areas of charge accumulation and the resistivity distribution. The measured self-potential anomalies are actually the potential drop caused by the current flow through the ground between the observation points.

In reality these steps occur gradually and simultaneously until steady-state conditions are reached.

2.2.3 Self-potential measurements as a seepage monitoring tool

From the previous section one can draw the conclusion that the convection current will increase as the flow of water increases. It can in fact be shown that the convection current (J_{conv}) density is directly proportional to the hydraulic gradient ∇P (see e.g., Sill 1983):

$$J_{\rm conv} = L \nabla P$$
.

The constant, L, is known as the cross-coupling coefficient, and depends on the properties of the minerals and the ground water, as well as on the pore geometry.

From the above one could be tempted to draw the conclusion that increased amplitudes of self-potential anomalies on dams could be directly linked to increased seepage flow. Unfortunately, the situation is slightly more complex than that. An important cause of

increased seepage flow is internal erosion in the dam, causing an increase of the porosity and the hydraulic conductivity. The resulting removal of fines will also directly affect the electric resistivity and the cross-coupling coefficient. Things are further complicated by the fact that the resulting self-potential anomaly is directly dependent on the resistivity of the ground. Consequently, an increased self-potential anomaly could be equally well explained by an increase in L, an increase in the resistivity, or an increase in the fluid flow.

To effectively use self-potential data for monitoring purposes, they should ideally be complemented by data on resistivity and hydraulic conditions. A self-potential anomaly taken on its own is fairly inconclusive. On the other hand, an increased self-potential anomaly not correlated with a resistivity change or a change in hydraulic head could well indicate an area with seepage problems. One should bear in mind, though, that there is also a regular seasonal variation of the self-potential anomalies. Such variation is generally not associated with anomalous seepage, although areas of exceptional seasonal variation could indicate seepage problems.

3 Monitoring installations at Hällby

3.1 The embankment dam

The embankment dam at Hällby power plant was taken into operation in 1970. It is located in the Ångermanälven River in the middle part of Sweden. The power plant and the spillway are located in the central part of the old river section, see Figure 2. Two embankment dams (called the left dam and the right dam) connect the spillway and powerhouse to the abutments. The dams, as well as the power plant and spillway, are founded on rock. The maximum water level is +292m. The seasonal variations are normally less than 1 m.

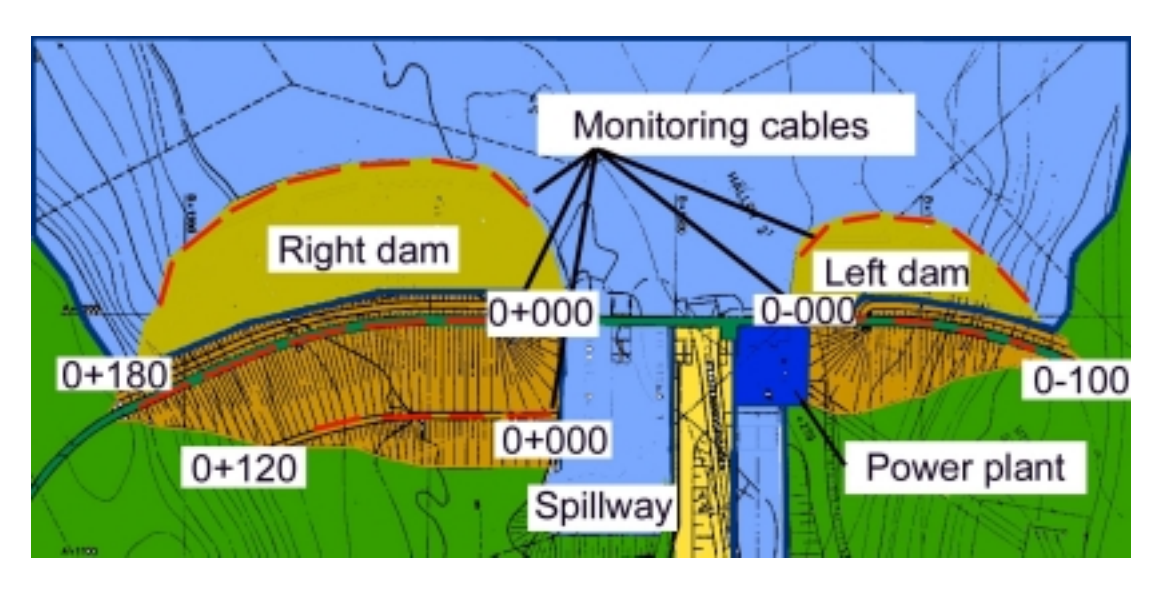


Figure 2 Plan over Hällby dam with monitoring sections (red dotted lines).

The dams are about 30m high and have a vertical central core of moraine, see Figure 3. The length is about 100m for the left dam and 160m for the right dam.

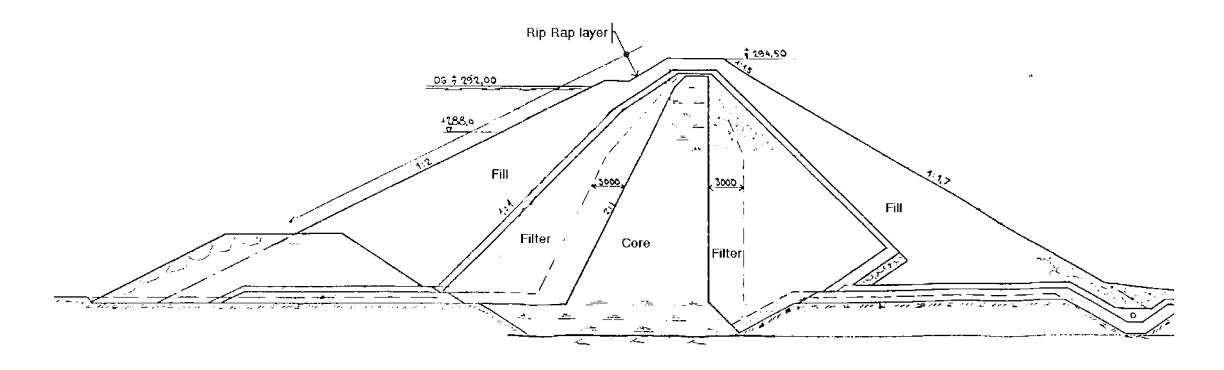


Figure 3 Hällby dam, cross section.

A sinkhole was observed in 1986 at the connection between the left dam and the power plant. Repair was performed in 1987 by grouting about 250m³ of cement-bentonite and silicate. A significant volume (150m³) was also grouted at the connection between the right dam and the spillway.

3.2 Installations

A multi-electrode data acquisition system developed at Lund University was used to obtain the resistivity data (Dahlin 1993; Dahlin 1996), in the first two dams using portable equipment. The monitoring system at Hällby is based on the ABEM Lund Imaging System, which is a further development of the equipment used at the first two dams. The modified system installed at Hällby consists of, an A/D-converter Lawson Labs AD201, a current transmitter Booster SAS2000, two switching units Electrode Selector ES464, a computer with a modem, and lightning protection.

Five cables are buried in the dam, buried immediately downstream the dam or placed at the upstream toe of the dam in the reservoir. Two cables are installed at the left side and three at the right side of the dam, as shown in Figure 4. The electrodes are buried at about 1 m depth, as indicated in Figure 5.

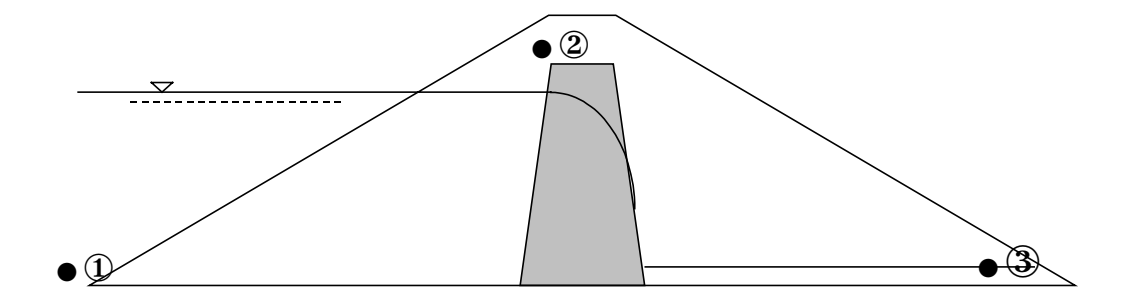


Figure 4 Sketch layout of the resistivity cable installation at Hällby.

- 1. Submerged resistivity cable located at the upstream side of the dam
- 2. Resistivity cable located at the crest of the dam
- 3. Resistivity cable located at the downstream toe of the dam

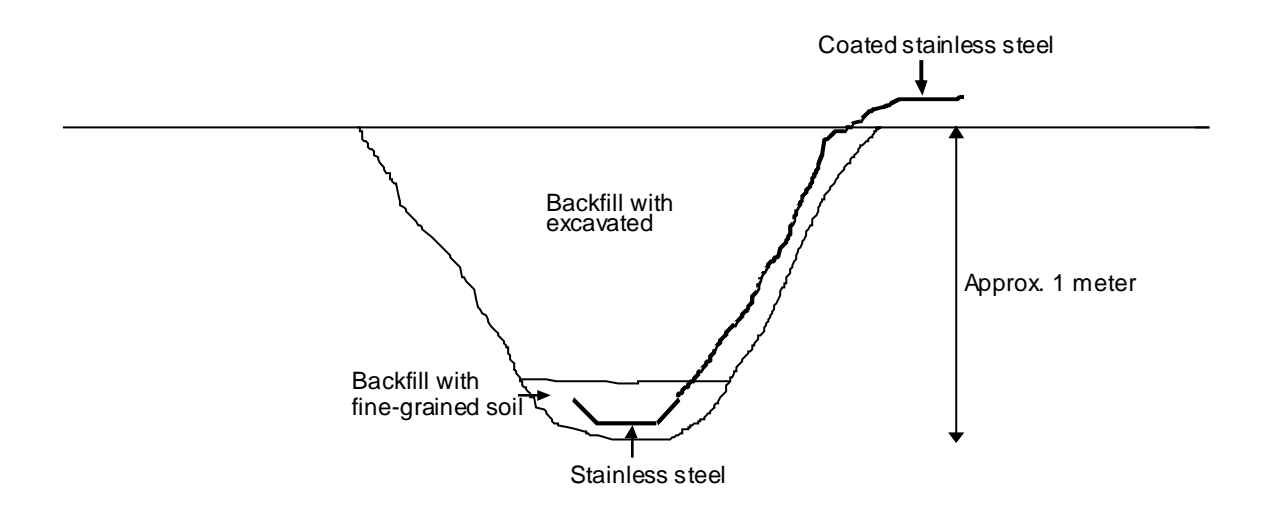


Figure 5 Sketch cross section of installation of the electrodes on land.

Table 1 Summary of the design of the electrode cables and electrode type, where the electrode take-out separation is 7 metres along each cable throughout. The planned cable no 3 could not be utilised due to the rough terrain on the left downstream side.

No:	Location	Cable type	Take-out & electrode type	No of take-outs	Active length /[m]	Blank cable/ [m]	Total length /[m]
1	Left crest	Land	Pig-tail + steel plate	16	105	65	170
2	Right crest	Land	Pig-tail + steel plate	27	182	154	336
3	Left downstream	-	-	(2)	-	-	-
4	Right downstream	Land	Pig-tail + steel plate	19	126	190	316
5	Left upstream	Under water	Pig-tail + ring	14	91	115	206
6	Right upstream	Under water	Pig-tail + ring	24	161	195	356
Total				100(+2)	665	719	1384

There are in total 102 electrodes installed on the dam (see Table 1), of which 43 are installed on the crest and 21 on the downstream toe. Stainless steel plates were used as electrodes on land (see Figure 6). The remaining 38 electrodes are installed in the reservoir on the dam upstream face, using underwater cables and ring electrodes in stainless steel (see Figure 7). The distance between each electrode is seven meters. This measuring layout gives a high flexibility and several types of resistivity measurements can be performed and the system is also used for monitoring of streaming potentials (SP).



Figure 6 Electrode and multi-core cable used on the dam crest and the downstream toe.



Figure 7 Electrode mounted on multi-core cable used on the upstream side.

3.3 Monitoring program

The data acquisition process is completely controlled by software, where the software scans through the measurement protocols selected by the user. The daily monitoring electrode configurations so far have been the combined Wenner-Schlumberger array and pole-dipole array (Figure 8), where the Wenner data was complemented with Schlumberger combinations in September 1997. Reciprocal Wenner-Schlumberger measurements are also carried out in order to assess the measurement errors. Initially, only n-factor 1 (see Figure 8) was used for pole-dipole measurements. In February 1999 the pole-dipole protocol files were expanded with measurements using other n-factors. Other configurations are also possible, but have not been used on daily basis.

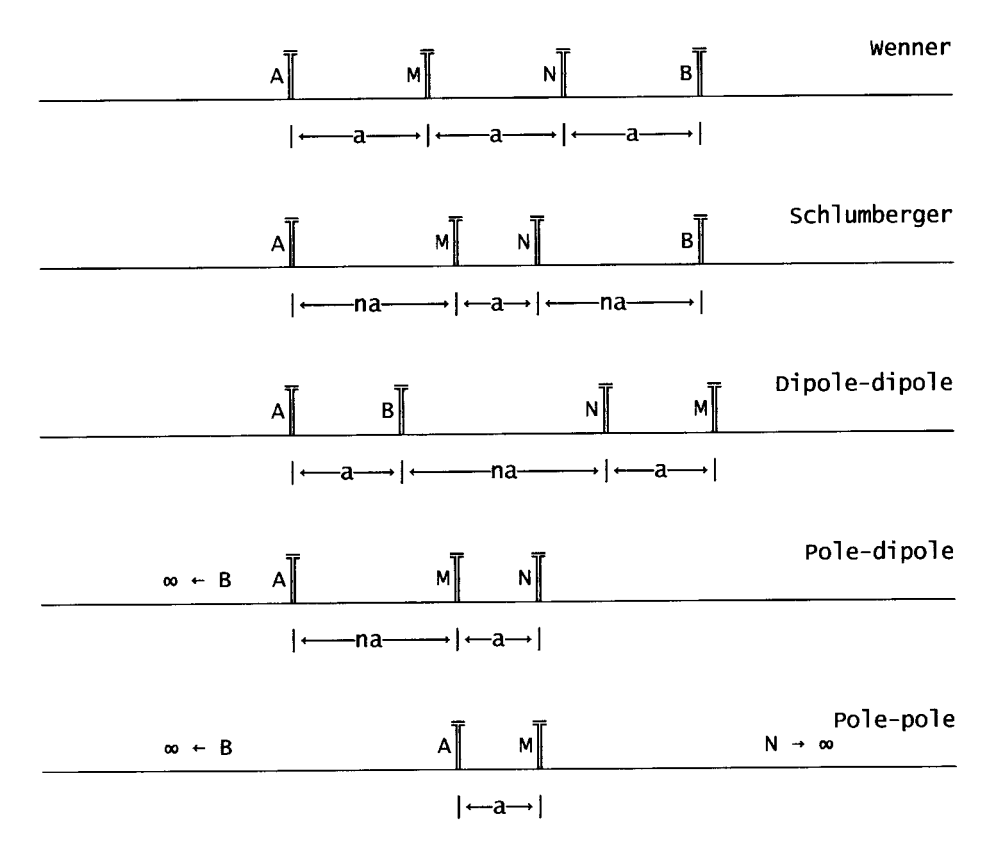


Figure 8 Example of different electrode array configurations (A, B = current electrodes, M, N = potential electrodes). For the pole-pole and pole-dipole arrays remote electrodes are employed.

In total around 3000 different data points are measured daily, distributed between the different lines and array types as shown in Table 2. The difference in number of data points between the different lines are due to the limitations imposed by the number of electrodes on each line.

Table 2. Number of data points in some of the different data sets measured on a daily basis at Hällby. Wenner-Schlumberger array with n-factor 1 is identical to Wenner array. In addition, reciprocal Wenner data are recorded (same number of data as Wenner-Schlumberger with n-factor 1).

	Pole-d	ipole	Wenner-Schlumberger		
Line description	Full ¹ n=1		Full ²	n=1	
Left crest	228	112	48	35	
Right crest	734	338	201	108	
Right downstream	336	162	78	51	
Left upstream	168	84	33	26	
Right upstream	564	264	147	84	

_

¹ Since 1999-02-26

² Since 1997-09-24

The data files are automatically compressed into a Zip-archive named after the present date on a daily basis. The data is transferred via modem for further processing and analysis.

3.4 Data processing and presentation

The measured data is processed by means of a time base filtering, where in particular 7-day or 15-day based median filtering is employed. Prototype software has been developed that automatically goes through the following procedure:

- Extract the desired data sets from the Zip-archives for a specified period (for example a year).
- Carry out a time base median filtering over a specified number of days (e.g. 15).
- Calculate a data file consisting of the all time median as the time base median of the whole period (for example a year).
- Convert all the time base filtered raw data files to the format used by the inversion software (see below). The all time median data section can be incorporated into each of the data file to allow time-lapse inversion.
- Create a batch control file for the inversion software Res2dinv and start the inversion.
- Extract the desired information from the inverted output files and save it in a format suitable for the continued processing and presentation.
- Scan through the inverted models and calculate statistical parameters for the whole period, such as annual median and mean resistivity sections, a section showing the variation coefficient, and sections showing the maximum and minimum interpreted resistivities of the period. A threshold for the mean model residual can be applied to filter away inverted model sections of too poor quality, which applies mainly to data recorded during the winter when the electrode contact resistances are highest and initially when the system was tuned in. When a threshold has been used it is indicated in the accompanying figure text in the following chapter.

The true resistivity structure is interpreted using the software Res2dinv, which does 2D smoothness constrained inverse modeling (inversion). A finite difference or finite element model of the resistivity distribution in the ground is generated, which is adjusted iteratively to fit the data so that the differences between the model response and the measured data (the model residuals) are minimized. This can be done either minimizing the absolute values of the differences (inversion with L1-norm or "robust inversion") or minimizing the squares of the differences (inversion with L2-norm or "smooth inversion"). The L1-norm is generally more stable towards noisy data, and tends to give models with sharper boundaries. The smoothness constraint prevents unstable and extreme solutions. In the inversion 2D structures are assumed, i.e. the ground properties are assumed constant perpendicular to the line of the profile, while the current electrodes are modeled as 3D sources (Loke and Barker 1996; Loke 1999a).

Time lapse inversion means that two data sets from different points of time are inverted together, where the first recorded data set would normally be regarded as a reference. In time-lapse inversion a smoothness constrain is applied not only on the spatial variation but also on the temporal variation between the data sets. This approach has been shown to focus the difference between the data sets on the actual change in the model and suppress artifacts due to the resistivity structure (Loke 1999b). As this is a new option for the inversion, the inversion parameters used for the time-lapse inversion have not yet been optimised for the type of data processed here. Thus, it is quite possible improved results may be achieved by adjusting the inversion parameters.

In dams, the resistivity can be expected to vary in a cyclic manner over the year, and hence some average of the variation over the year may be used as a reference data set. In the work presented here, the median over the selected period (one or more years) was used as reference data set, against which all the 7-day or 15-day median data sets were constrained in the inversion.

3.5 Data quality assessment

The data quality is assessed by measuring both normal and reciprocal data for the Wenner-Schlumberger measurements. Reciprocal measurements are carried out by using the potential electrodes for transmitting current and vice versa. In theory, this should give identical results, and differences are due to measurement errors. Thus, the measurement errors are estimated through calculating the observation errors as:

$$e_{obs} = 100 \cdot \frac{\left| R_{normal} - R_{reciprocal} \right|}{(R_{normal} + R_{reciprocal})/2}$$

where R_{normal} and $R_{reciprocal}$ are the measured resistances and e_{obs} the error in percent.

4 Results from resistivity measurements at Hällby dam

4.1 General experience

Daily data has been recorded since over three years from each of the five monitoring sections with resistivity, and since two years with SP. However, data is missing during some weeks in the summer 1998, when the lightning protection system was triggered by service activities that affected the power supply of the data acquisition system.

The quality of the daily data have so far been unsatisfactory for the land based electrode layouts, with sometimes a large scattering between the daily measurements, whereas the underwater electrodes mostly provide data of excellent quality with occasional disturbances (see Table 3). The mechanisms behind this are still not fully known, but a major reason is the high electrode contact resistance for the land-based electrodes. The data quality is, however, improved by time base filtration, which gives good quality for the upstream and downstream profiles and reasonable but not good data quality for the left dam crest. For the dam crest on the right dam the data quality remains very poor also after the 15-day median filtering. It may be possible to develop more intelligent data processing, but it must be stressed that the best way to increase the accuracy is probably to improve the electrode contact allowing higher currents to be transmitted. As can be seen in Table 3 the 7-day median is sufficient for the left upstream side, whereas the longer filter results in significant further error reductions in the other cases.

Table 3 Observation errors calculated from normal and reciprocal Wenner-Schlumberger measurements for the period September 1997-October 1999, expressed as the mean and median of the mean errors for each data set.

	Raw data		7-day i	median	15-day median	
	Mean	Median	Mean	Median	Mean	Median
Left crest	7.6	3.3	3.6	2.7	3	2.5
Left upstream	0.7	0.3	0.3	0.3	0.4	0.3
Right crest	34.9	23.4	20.6	15.6	13.7	9.3
Right upstream	3.4	0.3	0.8	0.3	0.4	0.3
Right downstream	12	1.6	1.9	0.7	0.8	0.6

4.2 Reservoir

Resistivity and temperature in the reservoir are measured automatically since February 1997; i.e. it started six months after the main monitoring system was installed. Some manual measurements were however performed during the autumn 1996, (see Figure 9). The result is similar to previous measurements at the embankment dams at Lövön and Moforsen where a sinusoidal resistivity variation has been found in the reservoir water (Johansson and Dahlin 1998). The variation recorded at Hällby has a similar but less regular appearance. There is a larger variation in the resistivity during the winter season, when the temperature is constantly around 0° C, which indicates a significant TDS variation. A TDS variation may be caused by a higher degree of groundwater being

discharged into the river flow during the later part of the winter season. The short peaks might be explained by events of rapid snow melt or rainfall giving flows of surface water interrupting the pattern. Independent measurements with a different sensor would be valuable to confirm the observed variation and to rule out measurement errors.

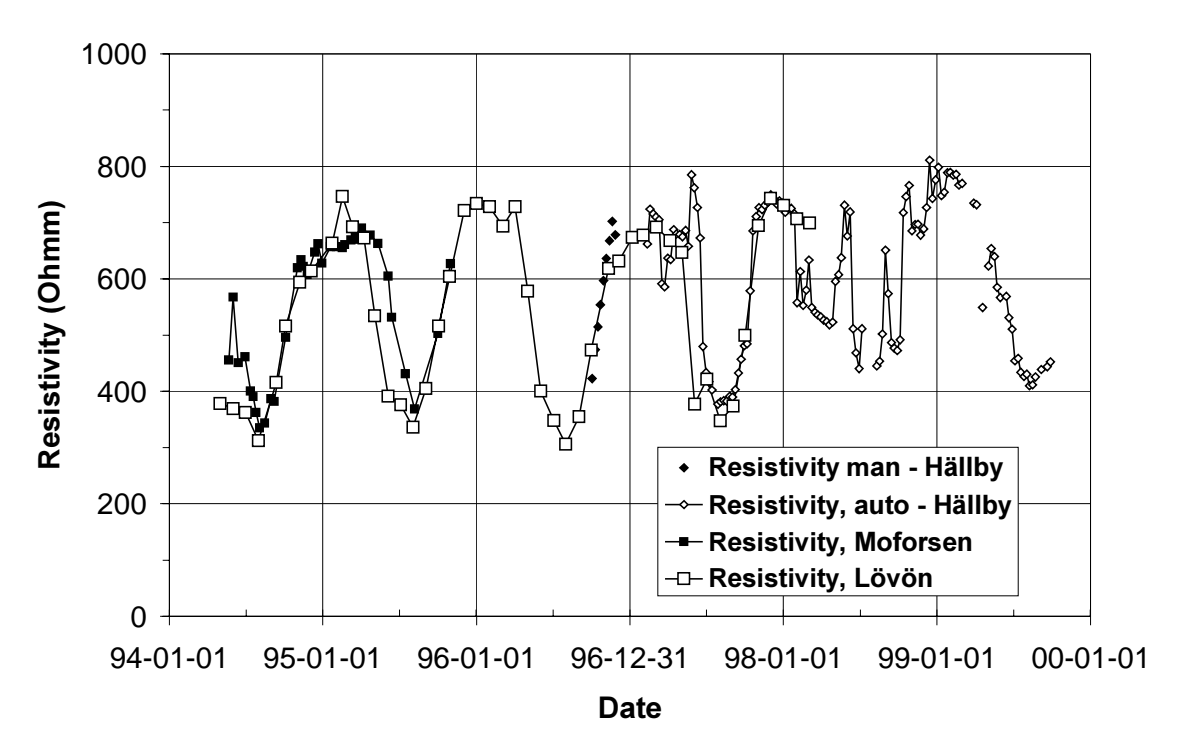


Figure 9 Measured resistivity in the reservoirs at Hällby, Moforsen and Lövön.

4.3 Left dam crest

Measurement errors from the monitoring from the crest are higher than desired using the Wenner-Schlumberger array, and can be expected to be at least as high for the pole-dipole array. The mean observation error (defined as the mean error of all measurements over the measuring profile) is 7.6% for the Wenner-Schlumberger array (see Figure 10). The data quality is improved to around 3% by using 7- or 15-day median filtered values as an input to the inverse modelling.

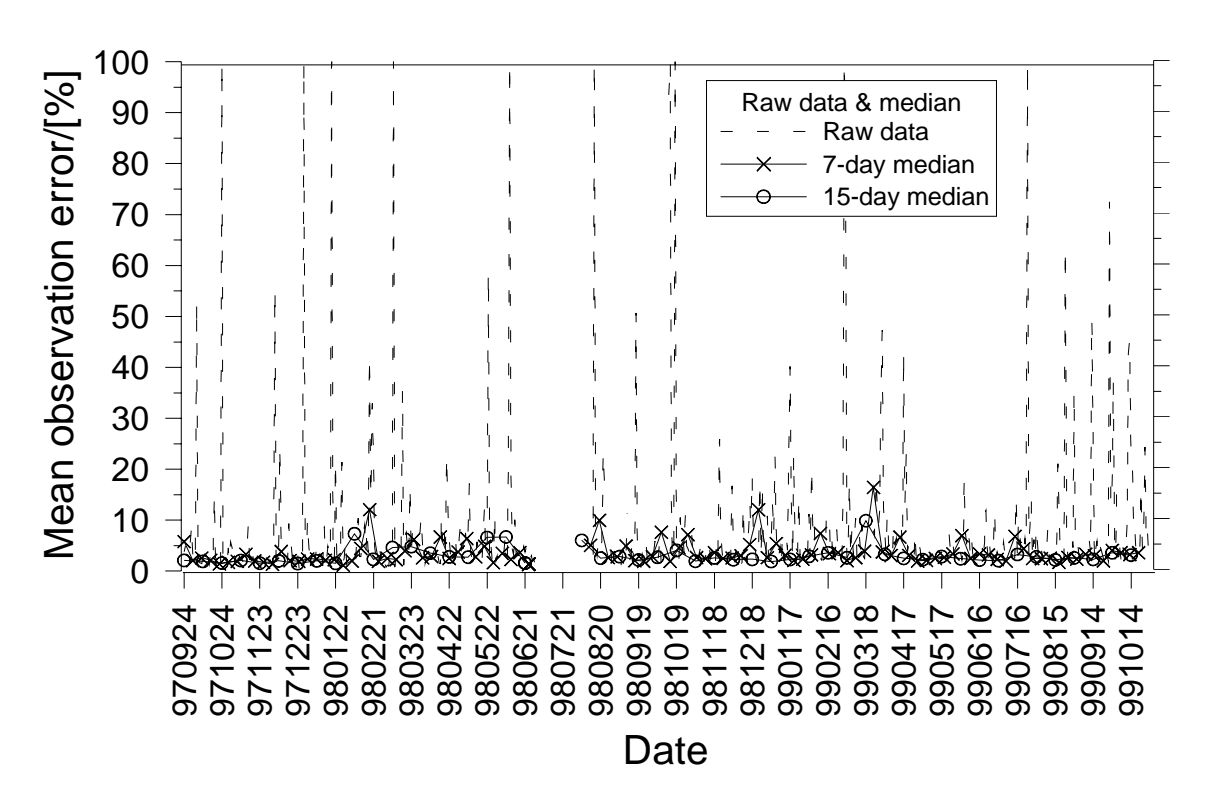


Figure 10 Mean observation errors from the Wenner-Schlumberger measurements on the left dam crest.

Despite the reduction in measurement errors, which have been estimated for Wenner-Schlumberger data only, the model residuals for the inverse modeling are rather high for the Wenner-Schlumberger data and very high for the pole-dipole data (Table 4). The pole-dipole data has been analyzed and found to be very stable from day to day, at least in warmer parts of the year. However, there are very strong contrasts in apparent resistivity in the data, as shown in the example for the pole-dipole array in Figure 11, so the high residuals may be a numerical problem.

Table 4 Model residuals in percent for inverse modelling of data from left dam crest (PD = pole-dipole, WS = Wenner-Schlumberger, L1 = inversion with L1-norm, L2 = inversion with L2-norm).

Left crest	PD-L1	PD-L2	WS-L1	WS-L2
Median:	20.9	34.4	5.4	9.9
Mean:	24.8	39.6	6.1	11.0
Max:	205.9	326.9	10.3	20.3
Min:	14.2	24.2	3.3	6.6
Time for min:	970201	970303	980830	990726
Time for max:	961118	961118	990127	981128

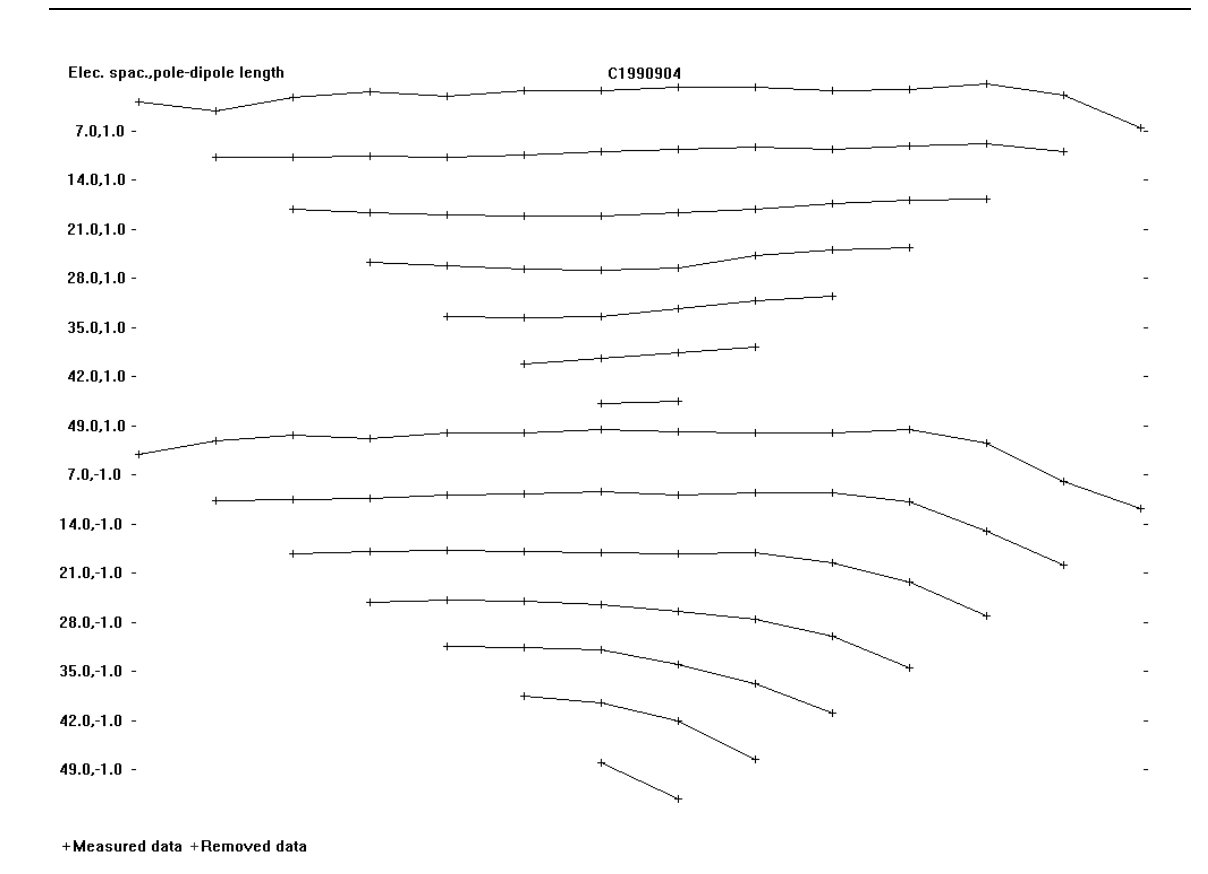


Figure 11 Example plot showing the relative variation of the forward and reverse pole-dipole data measurement at left dam crest (only data for the n-factor 1 shown).

In the model sections from the left dam crest the intake is situated at section 0m (right end of diagram), and the dam connects to natural ground in the left end of the section. The results from the inverse modeling based on pole-dipole measurements are shown in Figure 12, and the Wenner-Schlumberger model sections in Figure 13. Each figure shows the L1-norm as the upper plot and the L2-norm results as the lower plot. The presented sections are the median of all the inverted sections from 3 years. The general appearance of the inverted sections is similar, but details differ, and the L1-norm results tend to give higher contrasts as can be expected.

The upper six meters in the modeled section exhibit very high resistivities (many thousand Ω m), that are underlain by relatively low resistivities (some tens to a few hundred Ω m). Below the low resistivity zone the resistivities increase, which is only seen in the pole-dipole sections due to the smaller depth penetration of the Wenner-Schlumberger models.

The variation coefficients have a to some extent similar appearance between the array types, but with a significant difference between the L1-norm and L2-norm results (Figure 14 and Figure 15). The most significant difference is the high variation zone near the surface in the L1-norm version, which is not seen in the L2-norm sections.

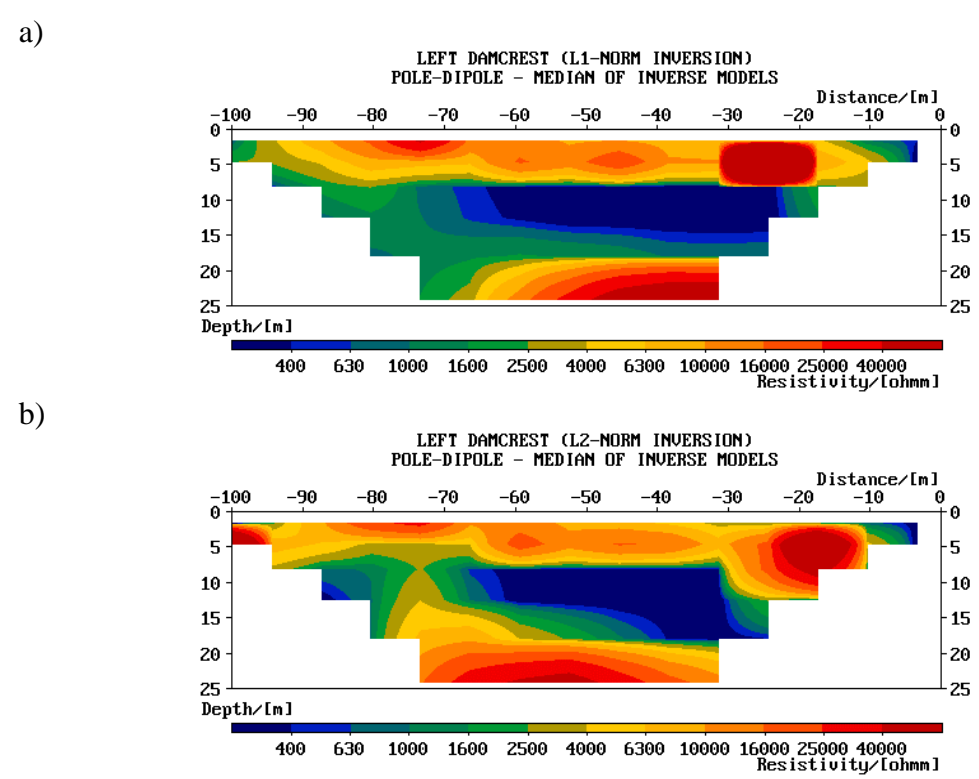


Figure 12 Median resistivity from inverse modelling based on 15-days median filtered poledipole measurements at left dam crest during 1996-1999. a) L1-norm inversion, b) L2-norm inversion.

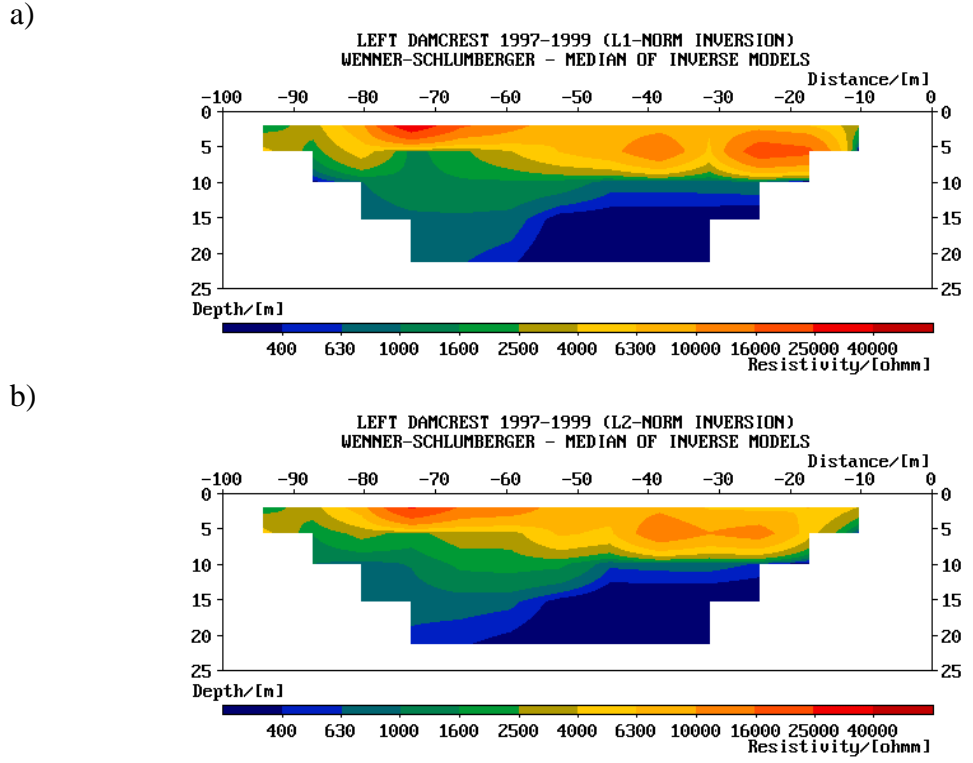


Figure 13 Median resistivity from inverse modeling based on 15-days median filtered Wenner-Schlumberger measurements at left dam crest during 1996-1999. a) L1-norm inversion (max model residual 35%), b) L2-norm inversion (max model residual 20%).

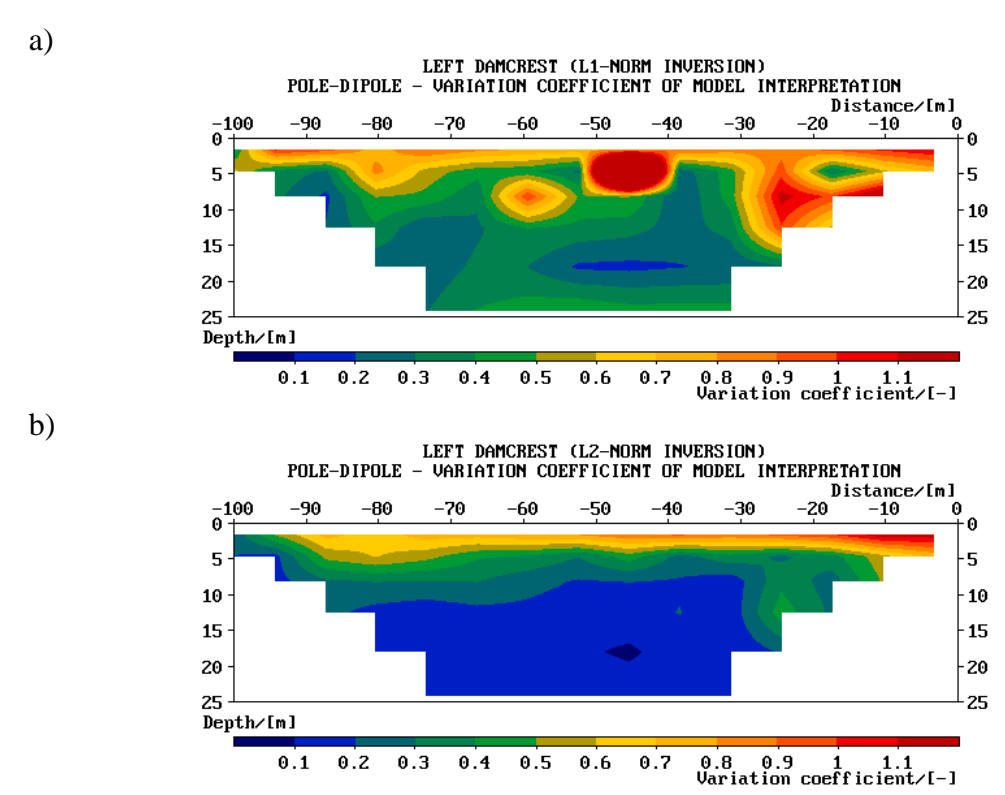


Figure 14 Variation coefficient from inverse modeling based on 15-days median filtered poledipole measurements at left dam crest during 1996-1999. a) L1-norm, b) L2-norm.

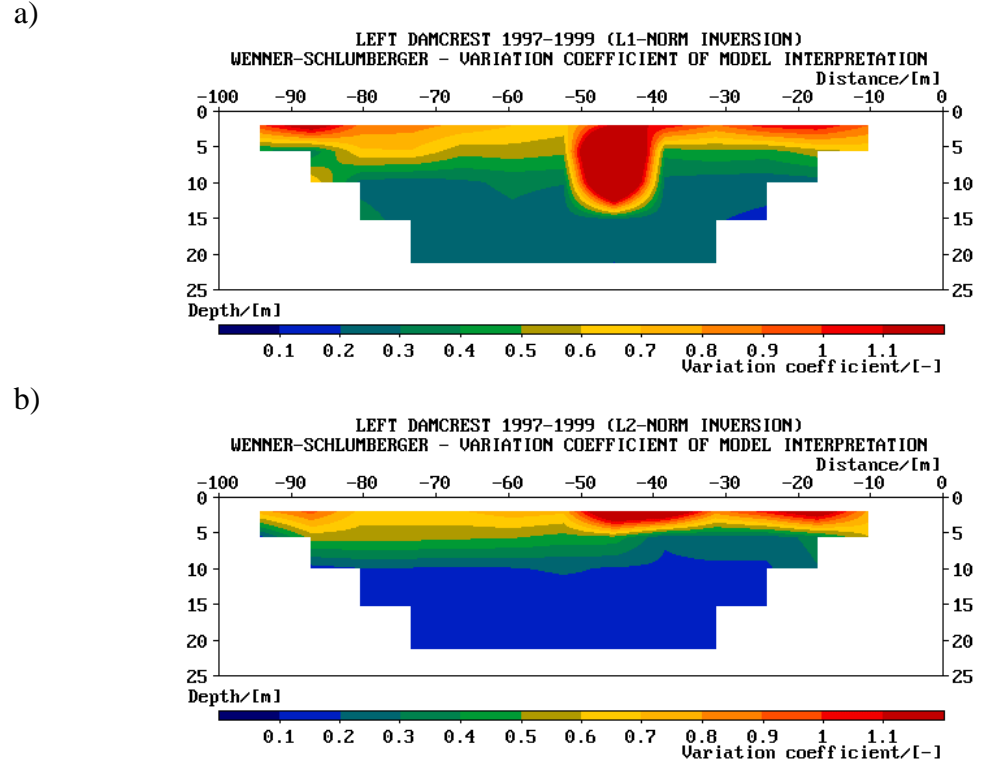


Figure 15 Variation coefficient from inverse modeling based on 15-days median filtered Wenner-Schlumberger measurements at left dam crest during 1997-1999. a) L1-norm, b) L2-norm.

4.4 Right dam crest

The result from the crest of the right dam shows the largest errors with a mean error of 34.9%, given by a general large error with many high peaks (Figure 16). Median filtering reduces the mean error to a mean of about 14%, which still is too large to be satisfactory. These errors imply that seepage evaluation is not meaningful to perform.

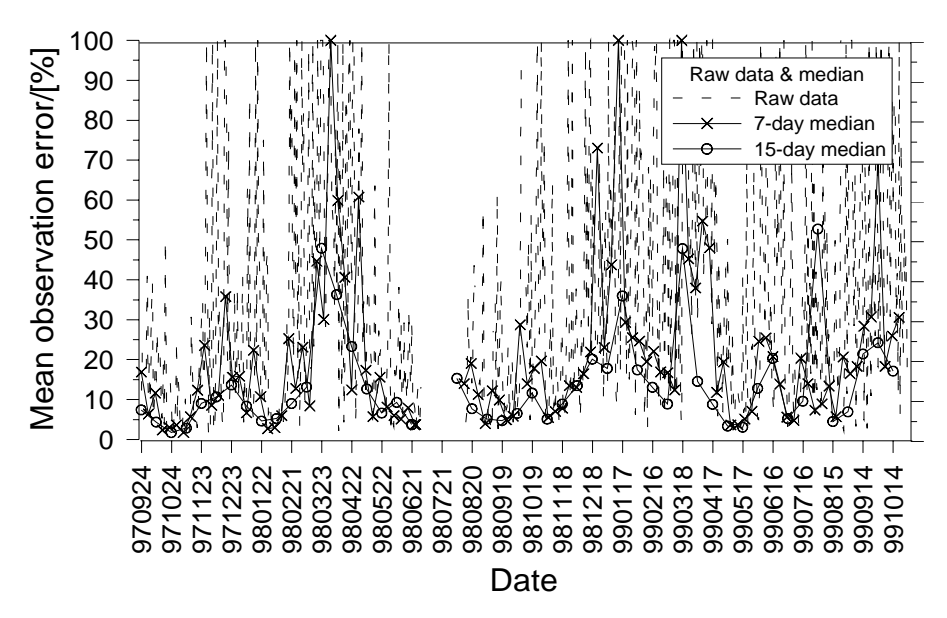


Figure 16 Mean observation errors from the Wenner-Schlumberger measurements on the right dam crest.

The model residuals for the inverse modeling are very high for the Wenner-Schlumberger data as well as for the pole-dipole data (Table 5). Only the minimum model residuals for the Wenner-Schlumberger array would normally be considered acceptable. This is not surprising considering the data quality problems experienced for the right dam crest. It may also to some extent be caused by large contrasts in the resistivities.

Table 5 Model residuals in percent for inverse modeling of 15-days median filtered data from right dam crest (PD = pole-dipole, WS = Wenner-Schlumberger, L1 = inversion with L1-norm, L2 = inversion with L2-norm).

Right crest	PD-L1	PD-L2	WS-L1	WS-L2
Median:	18.7	29.8	16.9	32.5
Mean:	24.6	37.4	23.5	34.9
Max:	102.7	158.9	120.2	106.1
Min:	8.9	19.5	4.9	9.7
Time for min:	970716	990721	990512	990527
Time for max:	990221	990221	990328	990328

The median of the whole period inverted section for the right dam crest display the same main characteristics for both the L1-norm and the L2-norm versions, and only the former is shown for both array types in Figure 17. There is a top layer of high resistivities, which is interpreted as being up to around 10 meters deep. Below this the

estimated resistivities drop, to reach below hundred Ω m in the outer ends and at depth, however there is a significant lateral variation in the resistivity distribution.

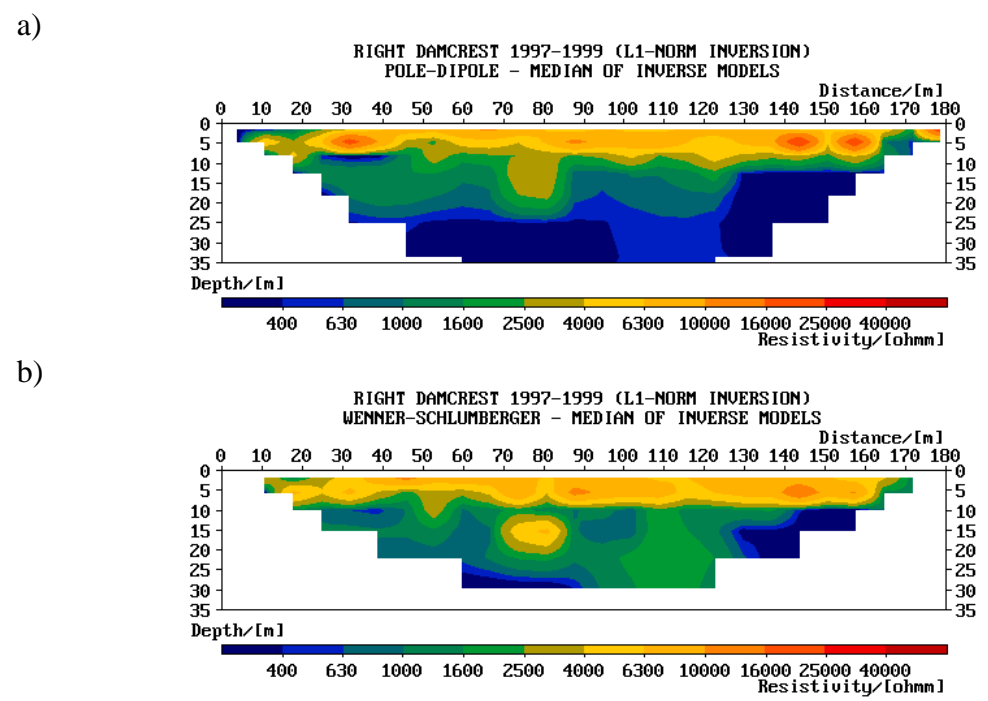


Figure 17 Median resistivity from L1-norm inverse modelling based on 15-days median filtered measurement data from right dam crest, a) pole-dipole during 1996-1999. b) Wenner-Schlumberger during 1997-1999.

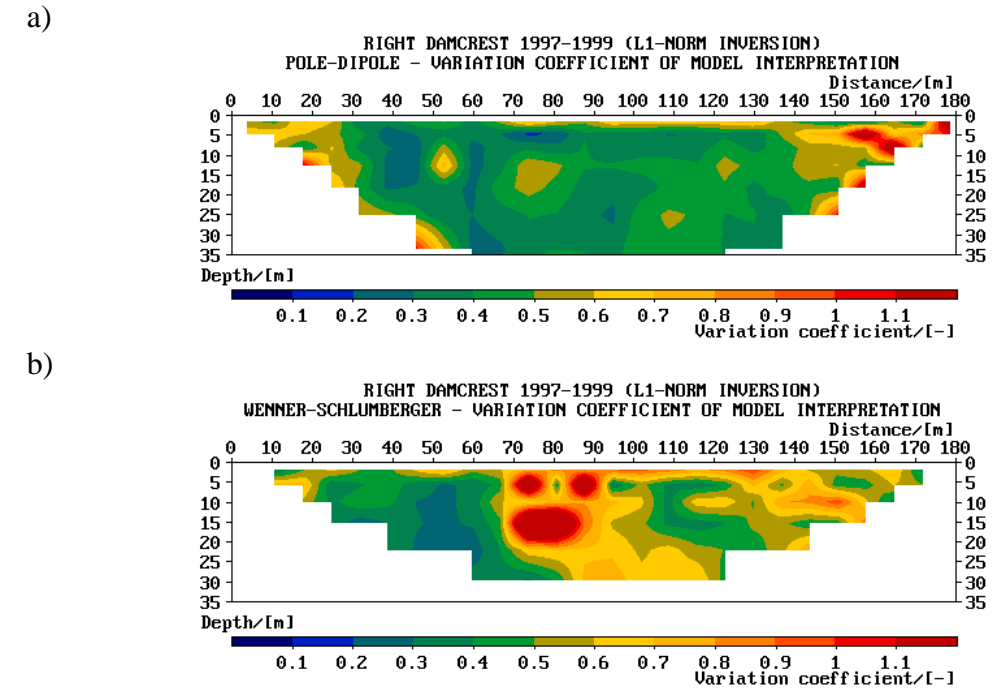


Figure 18 Variation coefficient from L1-norm inverse modeling based on 15-days median filtered measurement data from right dam crest, a) pole-dipole during 1996-1999

(max model residual 20%), b) Wenner-Schlumberger during 1997-1999 (max model residual 20%).

The variation coefficient of the L1-norm inversions for the right dam crest is shown in Figure 18. The patterns differ significantly between the different sections, and the sections also come out differently depending on what model residual value is regarded as maximum acceptable. The pole-dipole version is showing relatively little variation in the central parts, possibly as a result of many data sections being discarded as useless due to excessive model residuals. If the model residual threshold is raised above the 20% level used here for both array types, large variation occurs at the largest depths, which appears unrealistic. One common feature in the different sections is the high variation zone in the right part of the sections. The prominent zone centred around 80 metres distance in the Wenner-Schlumberger results (smaller zone present in the L2-inversion version) is only vaguely indicated in the pole-dipole section. Instead there is a high variation zone along the left edge of the pole-dipole variation coefficient diagram.

4.5 Downstream right dam

Higher data quality was obtained from the measurements at the downstream toe of the right dam (Figure 19). Although the raw data mean error is larger than that on the left dam crest it is mainly caused by isolated peaks. Median filtering reduces the mean errors to below one percent for the 15-days filtering period.

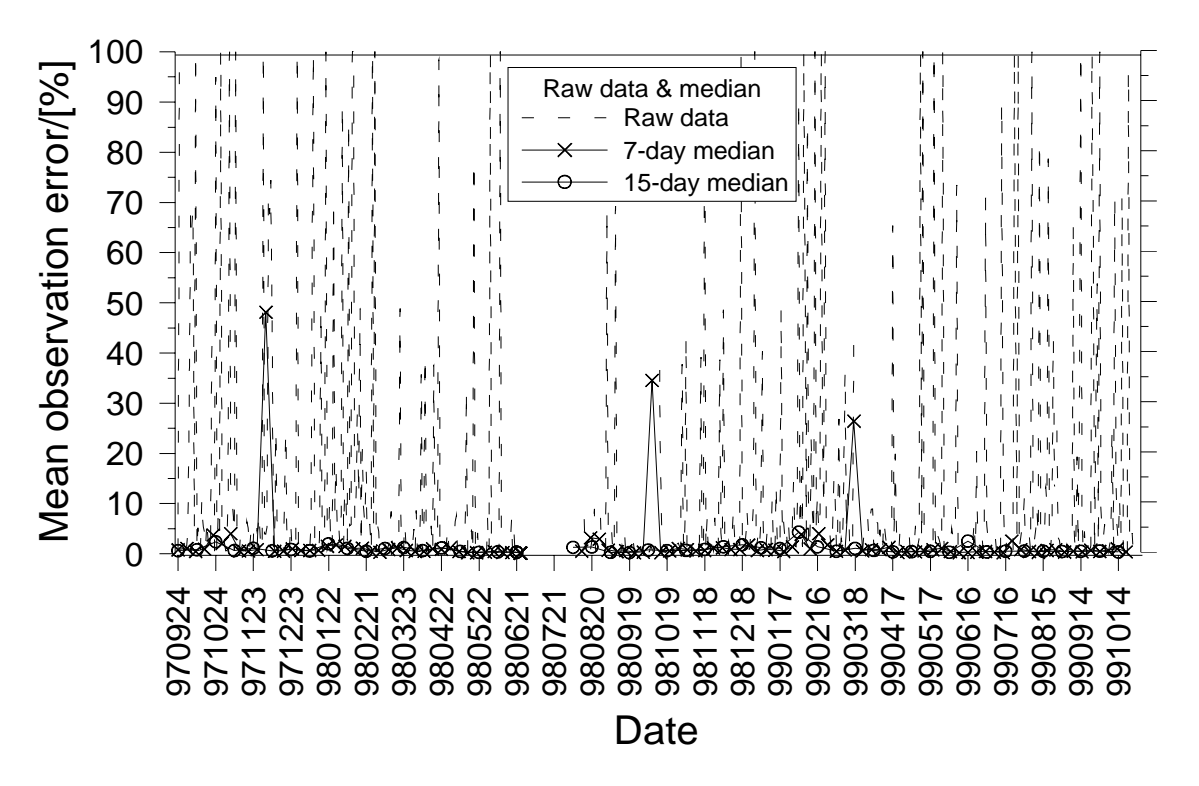


Figure 19 Mean observation errors from the Wenner-Schlumberger measurements on the right downstream side.

The higher data quality is reflected in the lower model residuals obtained in the inversion of the data from the right downstream toe (Table 6). This is particularly true

for the Wenner-Schlumberger where the model residuals are good considering the rather high resistivity contrasts.

Table 6 Model residuals in percent for inverse modelling of 15-days median filtered data from downstream right dam (PD = pole-dipole, WS = Wenner-Schlumberger, L1 = inversion with L1-norm, L2 = inversion with L2-norm).

Right downstream.	PD-L1	PD-L2	WS-L1	WS-L2
Median	3.9	6.0	2.8	4.8
Mean	8.5	17.2	2.9	5.5
Max	141.2	310.2	5.1	9.8
Min	2.1	4.4	1.9	3.8
Time for min	990805	970716	980830	980929
Time for max	961118	961118	990226	990211

Resistivity data from the 15-days median were used as input to the inverse modelling. Good agreement in the general behaviour with a seasonal pattern was found both for pole-dipole (Figure 20) and Wenner-Schlumberger (Figure 21) measurement, although the absolute values differ. The figures show the median of all inverted pole-dipole sections from the downstream toe of the right dam. The resistivities in the upper 10 metres are mostly several thousands to tens of thousands Ω m, under which it drops to the range of one thousand Ω m.

The general appearance of the variation pattern is similar in all the variation coefficient sections for the right downstream side (Figure 22 and Figure 23), but the L1-norm results exhibit a larger variation. There is a large near surface variation that reaches interpreted depths of up to more than 10 metres in the left part, which is shallower in the right part of the sections. There are deep pockets of high variation up to around 40 metres, and centred around 60-70 metres and 90-100 metres, present for all the arrays and inversion versions. These are more expressed in the L1-norm sections for both array types. Below these depths the variation is indicated to be low.

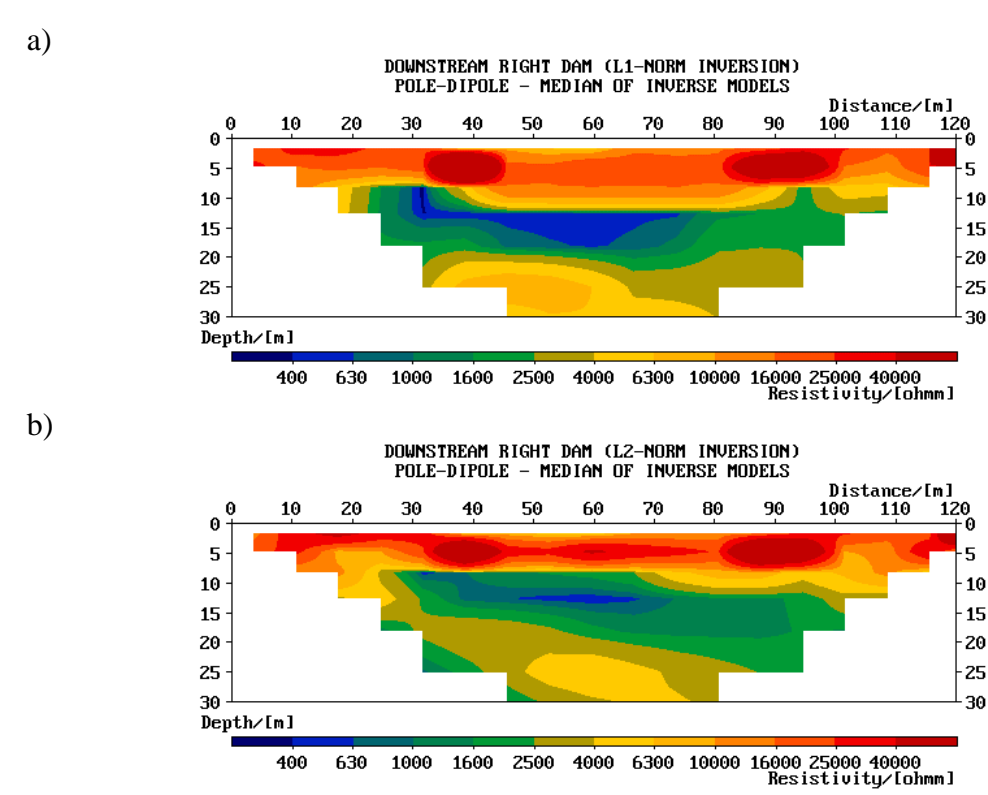


Figure 20 Median resistivity from inverse modeling based on pole-dipole measurements at right dam downstream side during 1996-1999. a) L1-norm inversion, b) L2-norm inversion.

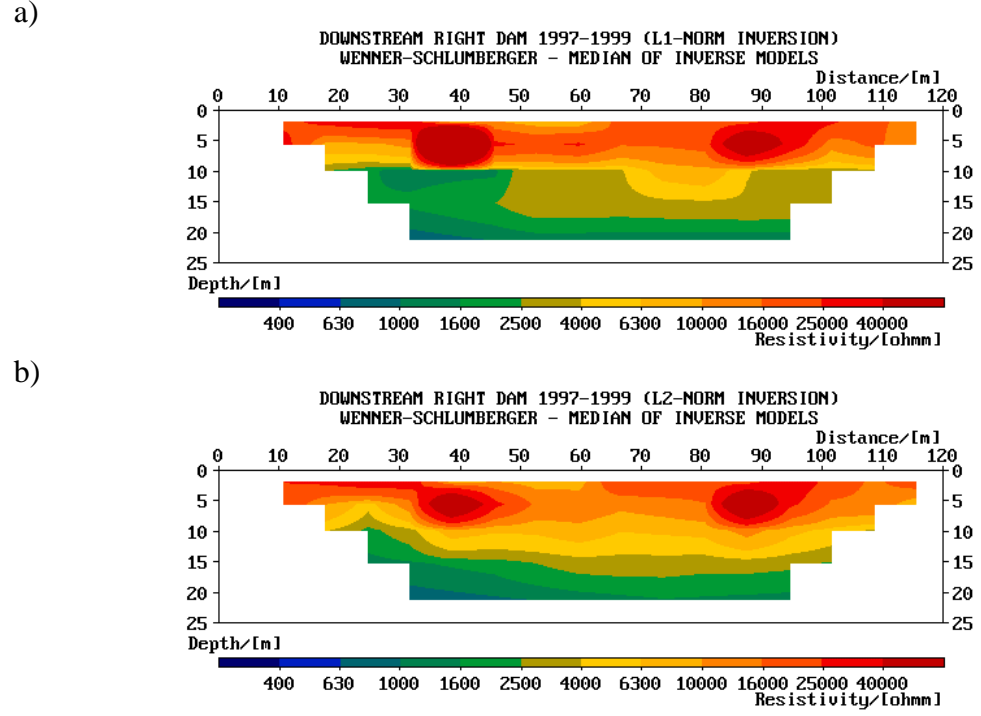
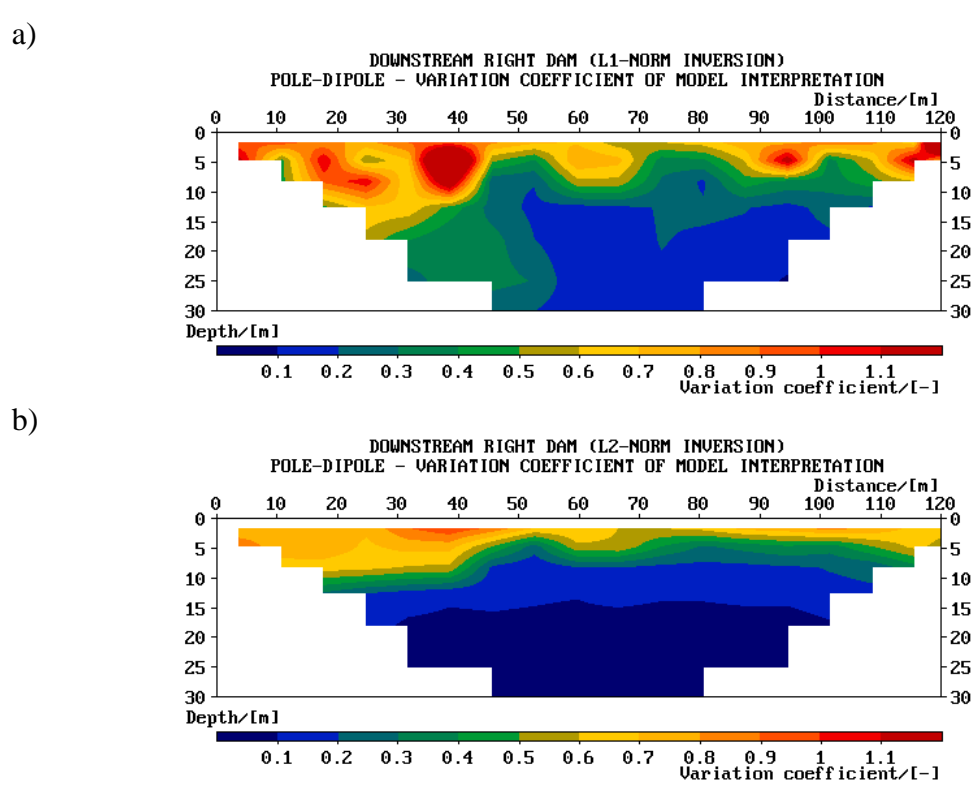


Figure 21 Median resistivity from inverse modeling based on Wenner-Schlumberger measurements at right dam downstream side during 1996-1999. a) L1-norm inversion, b) L2-norm inversion.



Variation coefficient from inverse modelling based on pole-dipole measurements at right dam downstream side during 1996-1999. a) L1-norm (max model residual 10%), b) L2-norm (max model residual 20%).

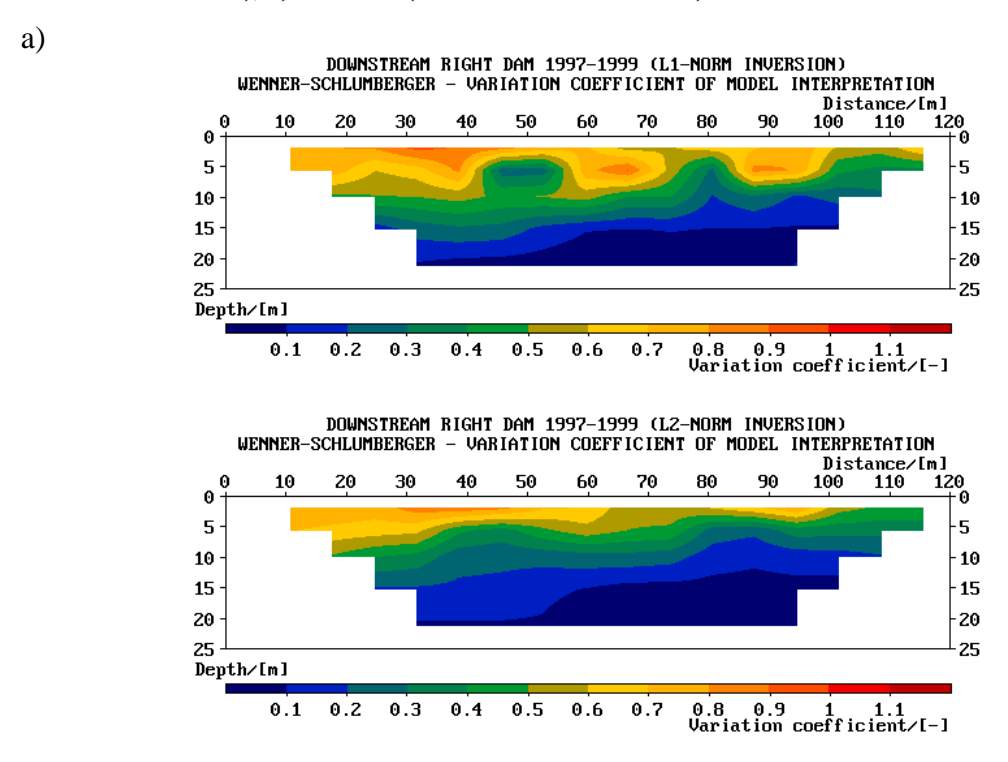


Figure 23 Variation coefficient from inverse modelling based on Wenner-Schlumberger measurements at right dam downstream side during 1997-1999. a) L1-norm, b) L2-norm.

4.6 Upstream left and right dam

The monitoring on the upstream side of the left dam shows good result with measurement errors generally about 0.3%, as shown in Figure 24. No inversion of all the result has yet been made because it requires that the electrode locations be known with higher accuracy than today. Hence, no seepage evaluation was possible to perform.

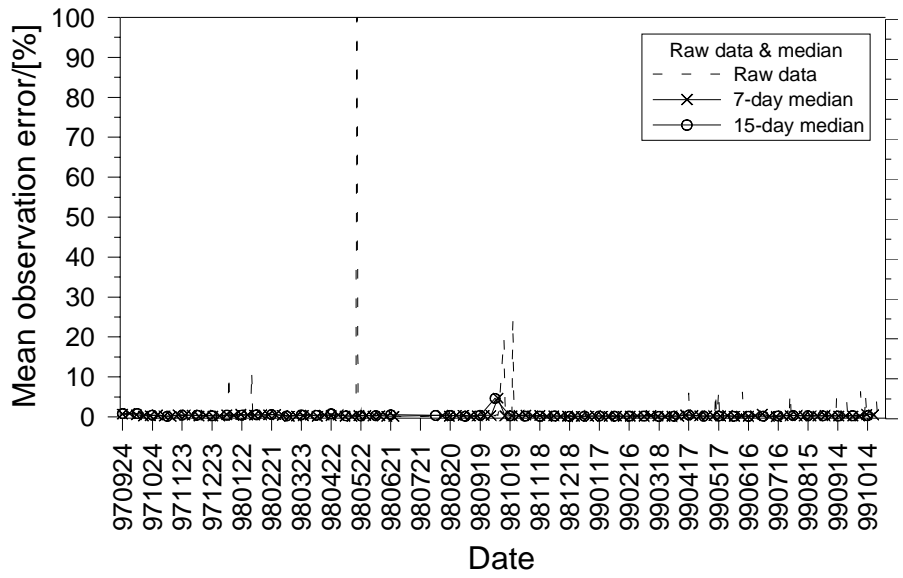


Figure 24 Mean observation errors from the Wenner-Schlumberger measurements on the left upstream side.

The data from the upstream side of the right dam is more disturbed than the left (Figure 25), which may partially be caused by noise picked up in the much longer lead-in on the electrode cable. As for the right downstream side the character of the noise is scattered peaks, which is efficiently removed by the median filtering resulting in mean observation errors below 0.5 % for the 15-day filter. However, it should be noted that much longer electrode separations are possible to achieve for the right upstream side than the left upstream side due to the larger number of electrodes. This means that measurements with smaller signal to noise ratio are included in the right dam measurements, which may also be part of the explanation.

The resistivity data measured upstream the left and the right dam at Hällby cannot be evaluated in a meaningful way yet, depending on the lack of information on the water depth above the underwater electrodes. The determination of the water thickness and the resistivity of the water is essential for the abstraction of meaningful data about the sub-bottom material, which is particularly true if the resistivity is significantly lower in the water than in the sub-bottom material.

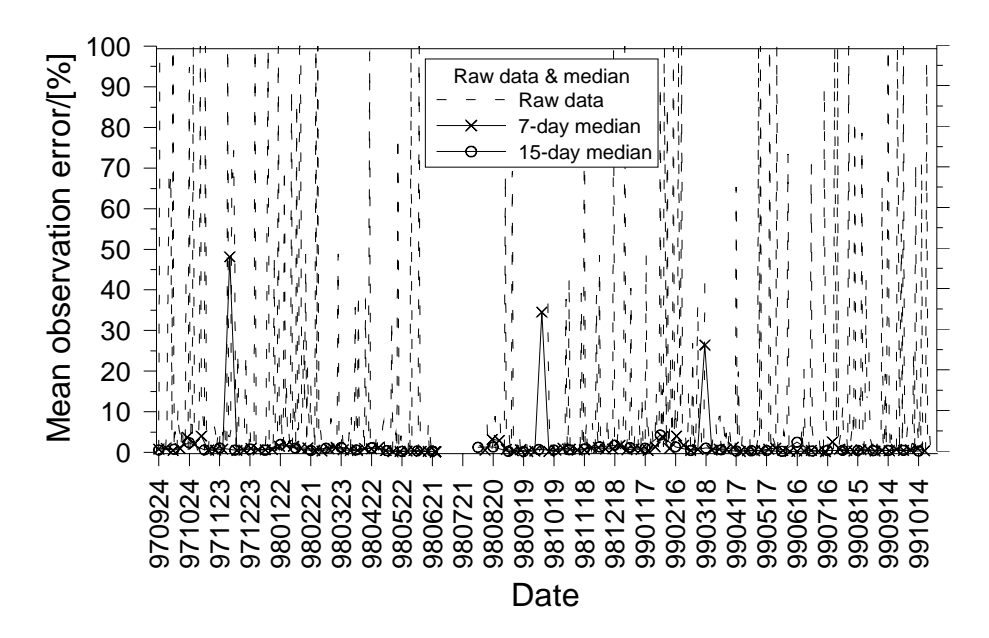


Figure 25 Mean observation errors from the Wenner-Schlumberger measurements on the right upstream side.

Figure 26 shows and example inverted section from upstream the right dam, where the water depth used for the modeling is a rough estimate based upon construction drawings and the approximate layout of the electrode cable. Errors in these depths will lead to very significant errors in the modeled section in a case like this. The low resistive area indicated to the right in the section might wholly or partially be caused by water depth errors.

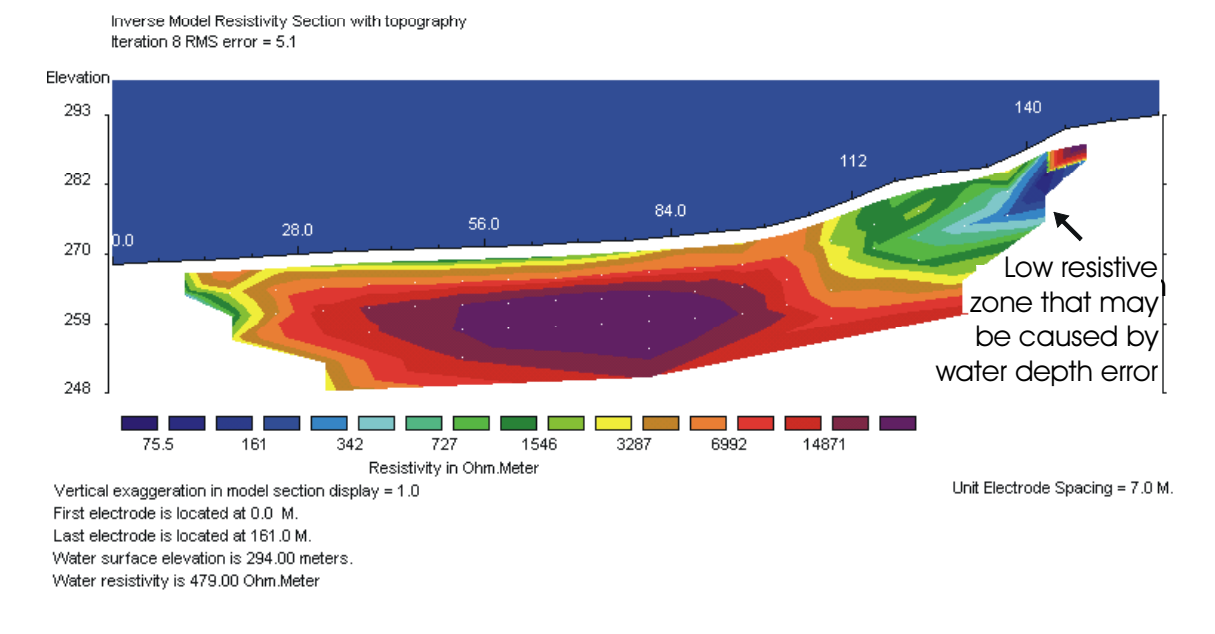


Figure 26 Inverted model section from data measured upstream the right dam. The water depth is a rough estimate based upon construction drawings and the approximate layout of the electrode cable.

5 Results from SP monitoring at Hällby

5.1 General

Self-potential data from Hällby are stable and apparently have good repeatability, although they were measured with stainless steel electrodes. Figures 13 through 17 summarize the SP-data collected over the first two years of monitoring. All were median filtered over a period of a week, and have reasonably low noise levels. Data from day 470 have been removed from all data sets as it exhibited clearly anomalous SP-values, indicating a possible system malfunction during that week. The time variation is generally fairly smooth and in several of the profiles there is a clear annual variation of the shape of the self-potential anomaly. The general appearance of the data is, however, slightly suspect. There is a prominent, very short-wavelength component in the data. Such fast spatial variations must be associated with very shallow sources. The appearance of such sources is quite unlikely and the potential variation is probably an effect of spurious electrode polarization caused by electrochemical interaction between the electrodes and the ground water.

The measured anomalies are the sum of a true self-potential component and an electrode polarization component, both of which appear to be stable and repeatable. The amplitude of the electrode polarization potentials can be roughly estimated by comparing the amplitude of the short and long wavelength parts of the anomalies. Such an analysis indicates that the amplitude of the polarization effect is comparable to that of the actual SP-anomaly in the land-based data. Data from the underwater profiles exhibit smaller polarization disturbances. The reason is probably that the underwater environment provides an electrically more stable and homogeneous environment for the electrodes. Differences in the properties of the electrodes cannot be ruled out, however.

Assuming that the polarization effect is randomly distributed along the profile, it then follows that a smoothed version of the anomaly curve should better reflect the true SP-anomaly. From such curves it should be possible to draw at least some general conclusions on the seepage through the dam. Below the mean SP-values calculated over the whole measuring period are used for this purpose.

5.2 Left dam

On the left dam SP-recordings were made along an underwater profile on the upstream side of the dam, and along a profile at the crest of the dam (see Figure 2). The distance along the profiles increases away from the intake. Figure 27 shows the data acquired during the measurement period. The top plate is a grayscale plot of the SP-values along the profile versus the day number, i.e., the individual profiles constitute vertical bands in the image. The middle plate is similar in format, but the mean profile has been subtracted from all profiles, the idea being to enhance small-scale variations and to try to remove some of the erratic variation along the profiles. The mean profile subtracted is shown in the bottom plate. The error bars in this plot were calculated including any annual variation, so the error bars cannot really be viewed as indications of measurement error. They are rather an estimate of the magnitude of the annual variation

of the SP-value at each station. In a homogeneous dam this variation would be equal for all electrodes. Consequently areas of higher annual variation could possibly indicate anomalous seepage conditions.

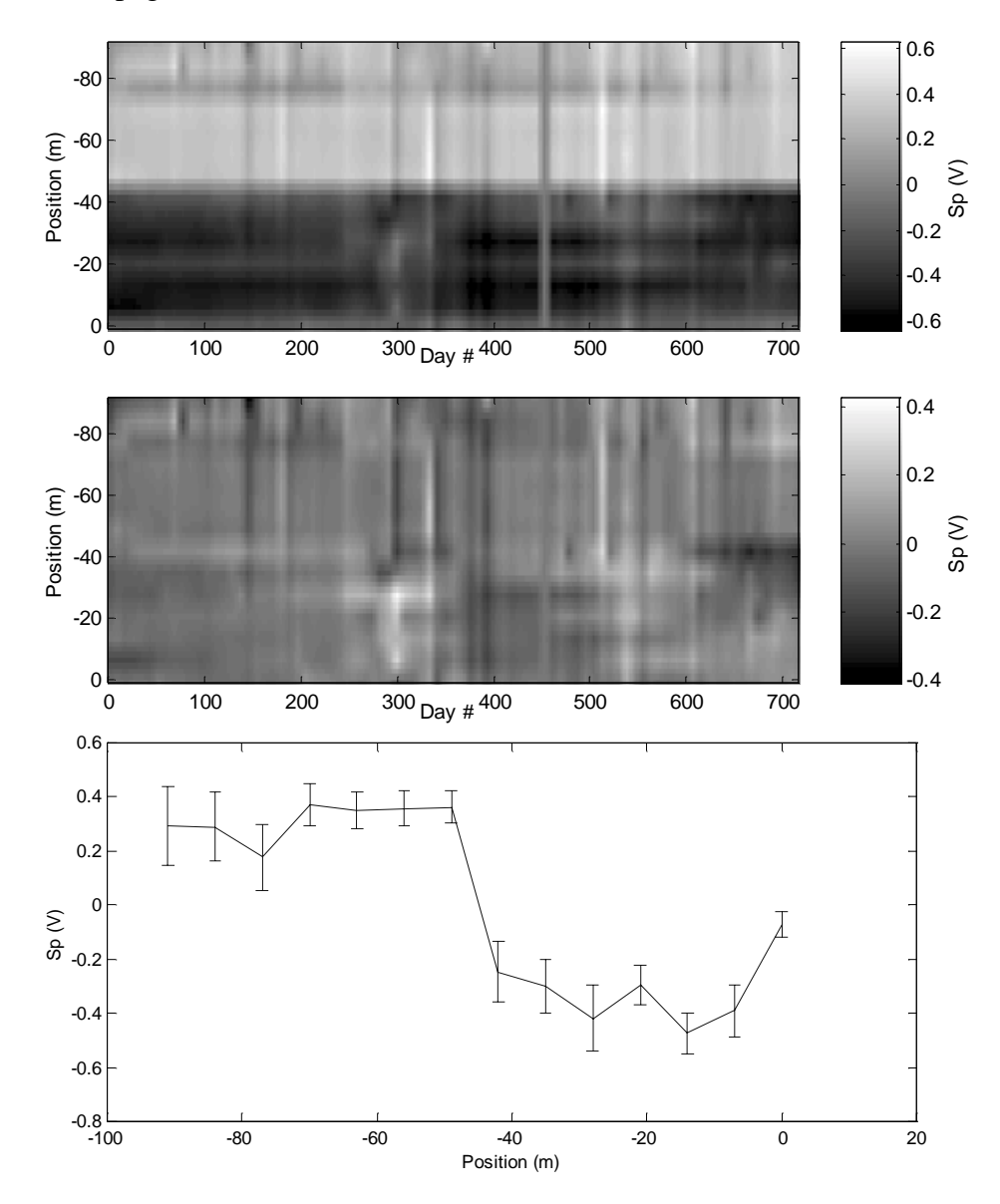


Figure 27 SP data along the profile on the upstream side of the left dam. Absolute SP (top), residual SP (absolute SP minus mean SP-profile) (middle) and mean SP-profile (bottom). The error bars show the estimated standard deviation, including the annual variation, during the period.

The SP-values vary strongly along the profile, around 700 mV over a distance of only several tens of meters. Such sharp horizontal gradients are not physically plausible and indicate that the measured SP-values are probably contaminated with spurious polarization potentials. The cause is probably a distinct change in local geological conditions, which would affect the polarization potential of the electrodes. The mean profile should be a good measure of this anomalous baseline, and by subtracting it from the data one should obtain a better picture of the true SP. The residual SP is fairly constant along the profile and exhibits virtually no annual variation. One can discern a

tendency towards higher variation for the parts of the later profiles closest to the intake and possibly a tendency towards more negative values for the latest recordings around the station at -40 meters. This could indicate an area of increased seepage.

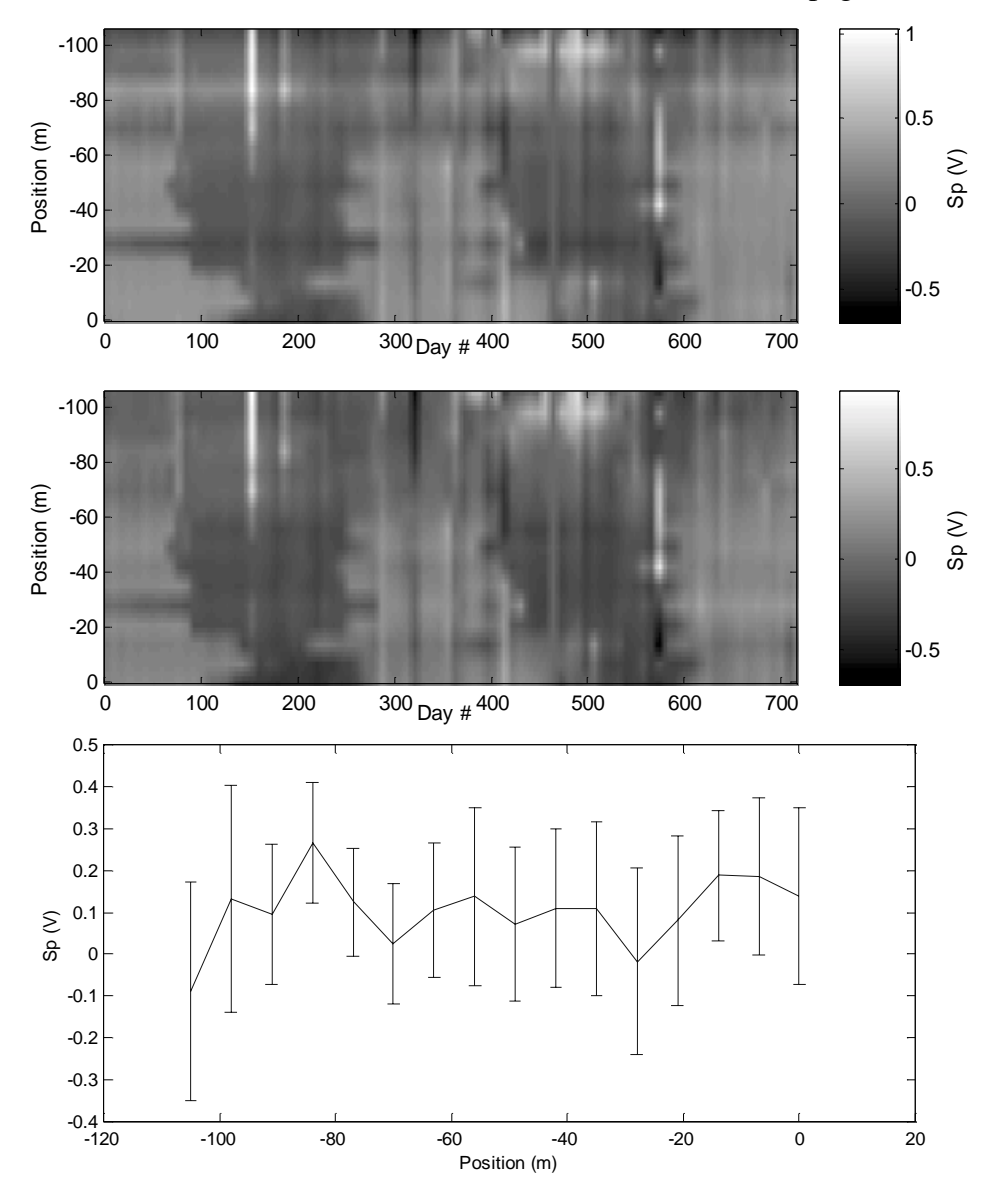


Figure 28 SP data along the profile at the crest of the left dam. Absolute SP (top), residual SP (absolute SP minus mean SP-profile) (middle) and mean SP-profile (bottom). The error bars show the estimated standard deviation, including the annual variation, during the period.

The SP data collected at the profile at the crest of the left dam is shown in Figure 14. Here the variation along the profile is more reasonable, but the horizontal gradients still appear unrealistically high, indicating a spurious station to station polarization potential variation. In contrast to the upstream data there is a significant annual variation. Since the mean profile is quite flat, the residual SP does not differ significantly from the absolute SP. There is only a slight decrease in the span of the data and in the station-to-station polarization noise.

5.3 Right dam

On the right dam SP-recordings were made along profiles on the upstream side of the dam, at the crest of the dam, and at the downstream side of the dam (Figure 2). The distance along the profiles increases away from the intake.

Figure 29 shows the SP-data from the upstream profile. Their characteristics agree well with those of the left dam upstream data. The polarization noise is significant, but it is also quite effectively suppressed in the residual SP. The annual variation is insignificant. One interesting difference is that the standard deviation increases with decreasing distance along the profile.

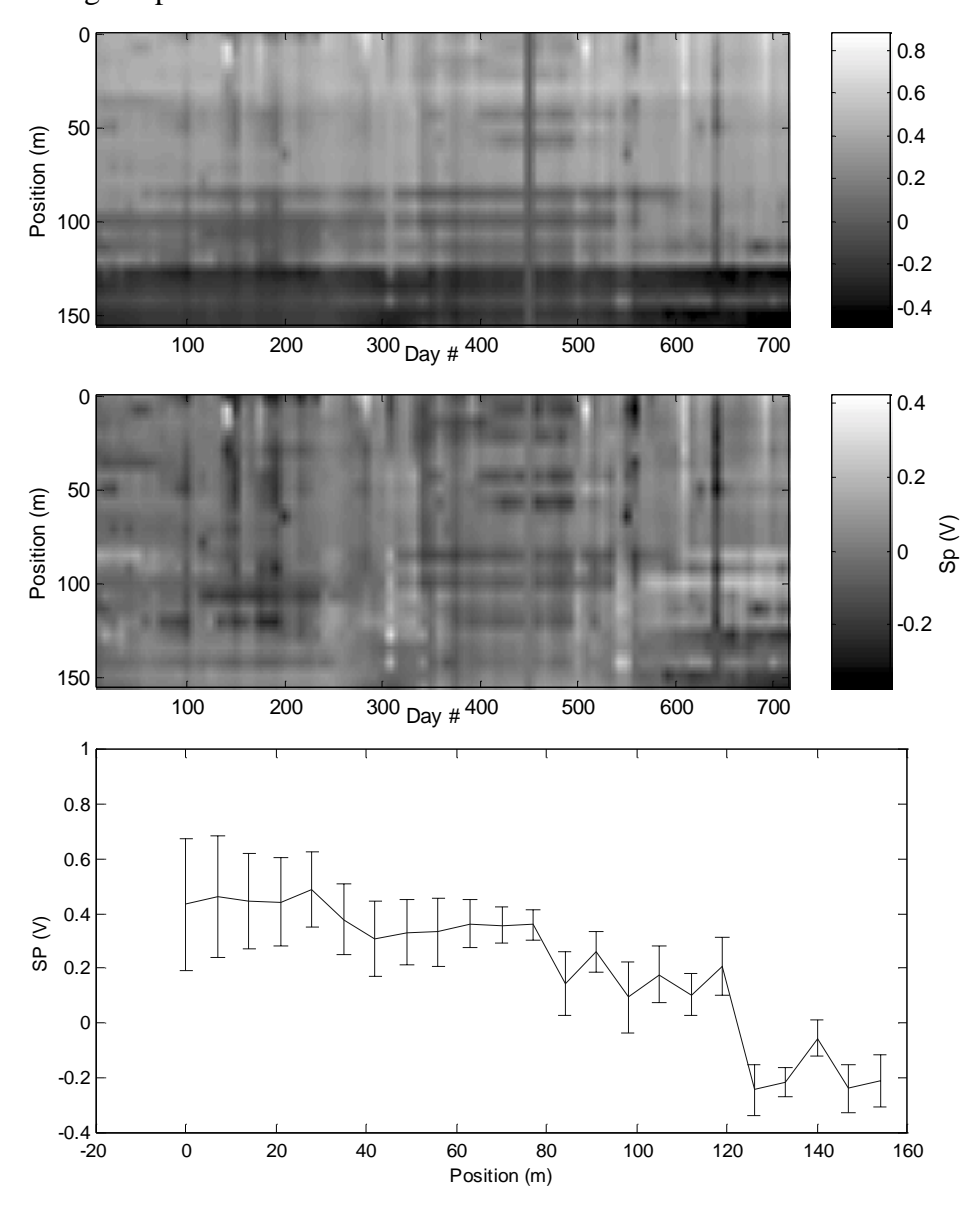


Figure 29 SP data along the profile on the upstream side of the right dam. Absolute SP (top), residual SP (absolute SP minus mean SP-profile) (middle) and mean SP-profile (bottom). The error bars show the estimated standard deviation, including the annual variation, during the period.

The SP-data from the crest of the right dam are shown in Figure 30. There is a significant noise component at the beginning of the profile. This noise is significantly reduced in the residual data. The annual variation is weak, but clearly visible, and stronger than in either of the upstream data sets. The standard deviation decreases slightly with decreasing profile distance.

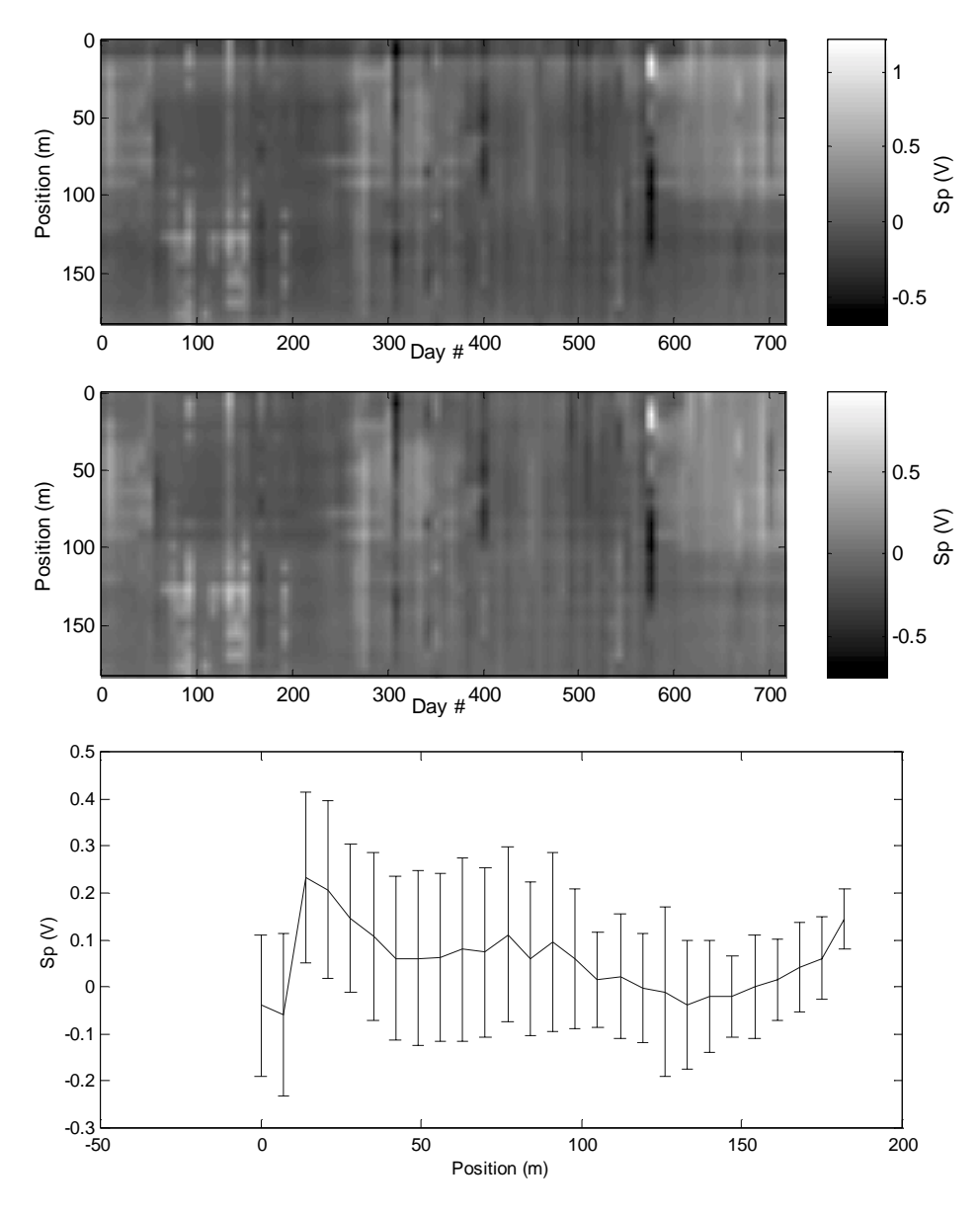


Figure 30 SP data along the profile at the crest of the right dam. Absolute SP (top), residual SP (absolute SP minus mean SP-profile) (middle) and mean SP-profile (bottom). The error bars show the estimated standard deviation, including the annual variation, during the period.

The downstream data, shown in Figure 31, are very similar in character to the data from the crest of the left dam. The annual variation is clearly evident. The standard deviation decreases with decreasing distance along the profile.

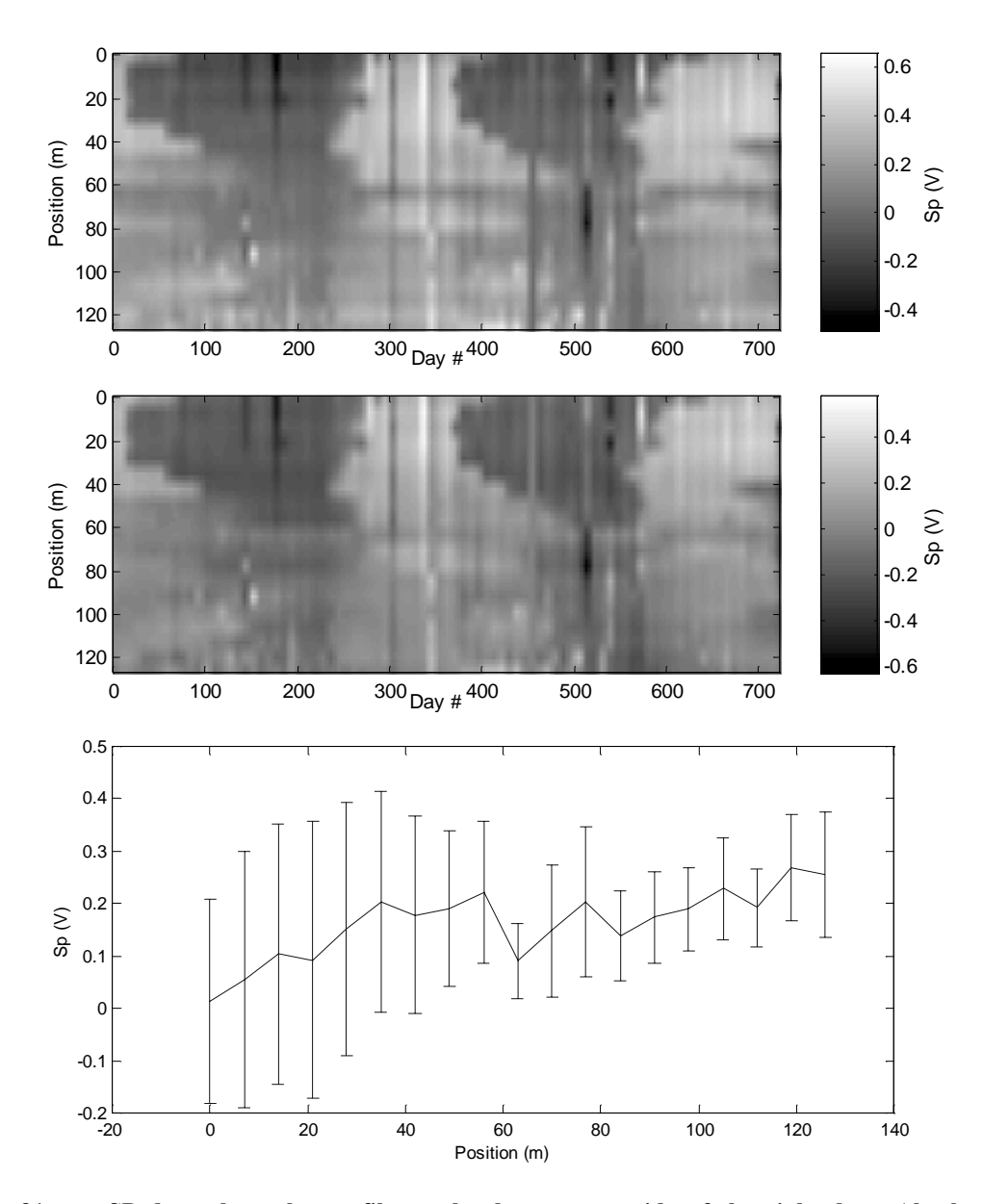


Figure 31 SP data along the profile on the downstream side of the right dam. Absolute SP (top), residual SP (absolute SP minus mean SP-profile) (middle) and mean SP-profile (bottom). The error bars show the estimated standard deviation, including the annual variation, during the period.

5.4 Summary and synthesis

The lack of annual variation of the upstream anomalies indicates that there is no significant variation in the strength and location of the streaming potential sources. This agrees well with the fact that the changes in reservoir water levels are minor, only on the order of 1 to 1.5 meters. Consequently the annual variation found in the land-based profiles must be attributed to changes in electrode polarization potentials, caused by annual variation of the local geological conditions in the vicinity of each electrode. It is most interesting to note that this variation also shows very high repeatability. The

magnitude of this polarization based annual variation appears to be comparable to the magnitude of the SP-anomalies.

Even though the polarization effects appear stable and repeatable, they are so large that it becomes necessary to try to remove them before attempting to interpret the SP-anomalies in terms of streaming potentials. A certain amount of reduction can be achieved by studying residual SP-data, but the ideal is of course to remove the noise at the source. Recent experiments at the Sädva dam, where both stainless steel and non-polarizeable electrodes are installed, have indicated that it might be possible to minimize the polarization effects by applying certain measuring techniques. This is still being investigated.

One would expect the SP to increase from the upstream area to the downstream area, as influx areas generally acquires a negative charge, and outflux areas a positive. This assumption is not really borne out by the comparison of all the profiles, shown in Figure 18. The reason is probably that polarization effects offset the zero levels differently for each profile, and is a further indication of the importance of minimizing these effects.

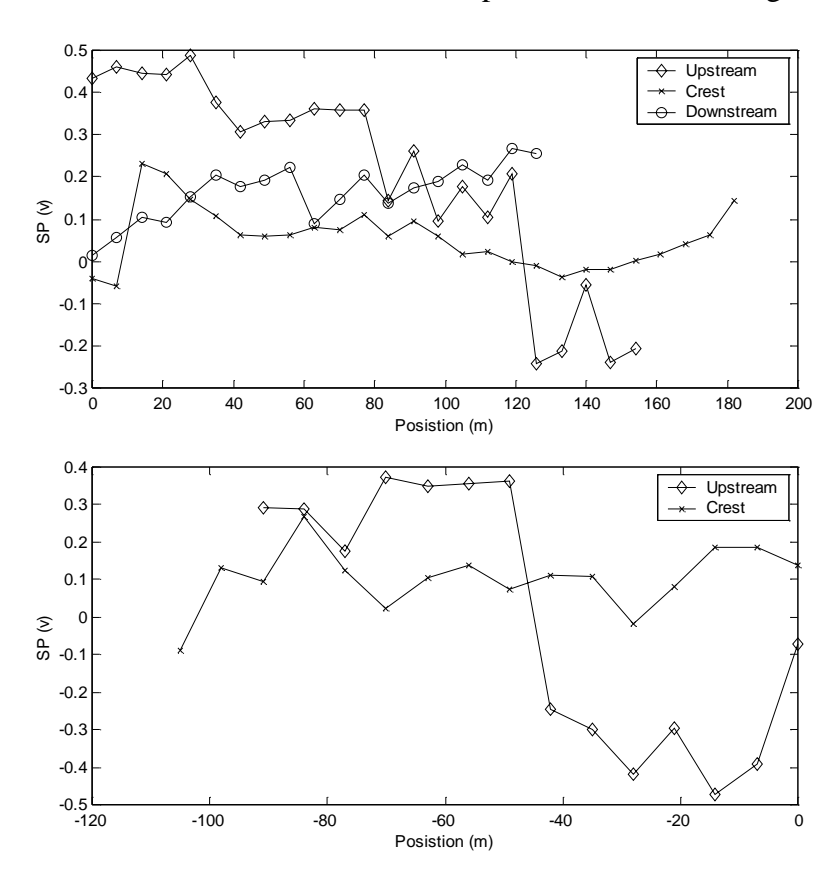


Figure 32 Comparison of mean SP-profiles. Note that the position along the profile is not corrected for the starting position of the profiles, so the plots should be used for general observations only.

6 Temporal resistivity variation and seepage evaluation

6.1 General

A seepage evaluation requires resistivity data of excellent quality. Data obtained from the time-lapse inversion seems to improve the result compared to previous inversions (Johansson, and Dahlin, 1996 and 1998). At least data from the left dam crest and from right dam downstream seem to have such credibility as they can be used for some seepage interpretation. The data quality does not allow automatic evaluation even though the Wenner-Schlumberger data seem to be close such a quality. Data from the right dam crest is still not good enough for any attempt for seepage analysis.

The basic evaluation is based on the temporal resistivity variations. As discussed above several factors can cause seasonal variations, especially in the shallow parts of the monitoring sections. The main problem is thus to separate those undesired variations from the seasonal variation that is caused by the seepage flow.

The basic input for the seepage evaluation is the resistivity variations in the reservoir. Maximum resistivity occurs normally in December/January, as showed above in Figure 9. In the evaluations below that the maximum value occurs in January 1st and minimum in July 1st. Seepage evaluation has been made based on the methods described in section 2.1.4.

6.2 Left dam crest

Calculated resistivities from the both Wenner-Schlumberger and pole-dipole measurements show stable result, with a significant seasonal variation. The most reliable result seems to be obtained using the L2-norm, however this needs confirmation from numerical modeling and analyses. The general behavior of the variation depends on the depth – the maximum value occurs earlier at smaller depths and with larger variation.

The resistivity as well as the variation exhibit larger values close to the surface, see Figure 33 and Figure 14. The maximum values at d=1.8m (mean value) can be explained by the freezing, which not is the case for the deeper evaluation cells. However, some influence from freezing or at least low temperature is probable present also at d=5.4m.

The result from the pole-dipole-measurements (Figure 34) is similar to Wenner-Schlumberger. A seasonal variation occur in the upper part is probably caused by freezing. In the deeper part (below at d=8m) is the variation probably caused by seepage induced variations.

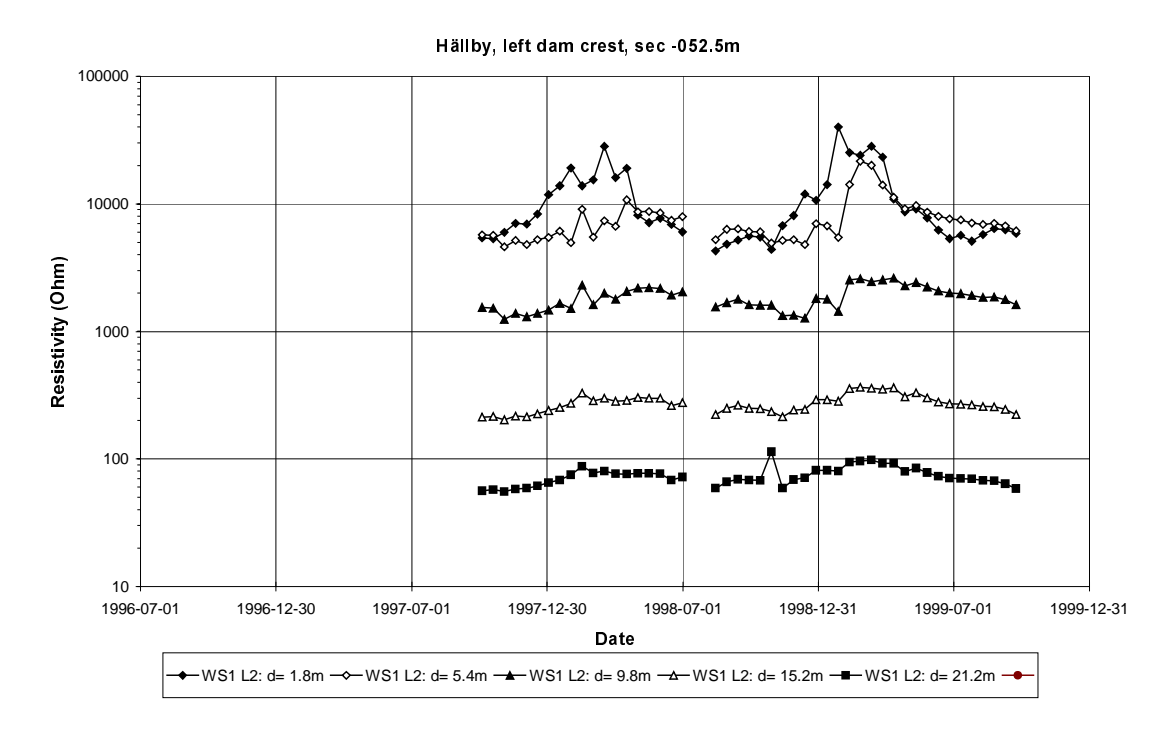


Figure 33 Evaluated resistivity using L2-norm at section 0-052.5 at some depths, from Wenner-Schlumberger measurements.

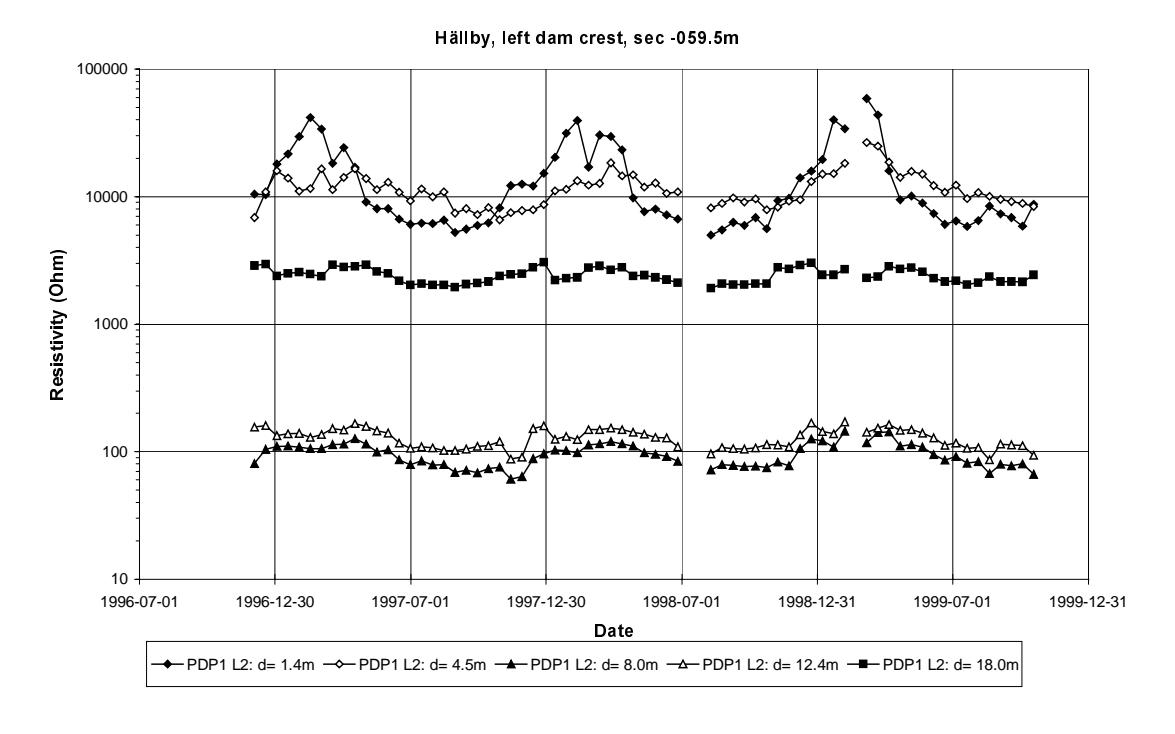


Figure 34 Evaluated resistivity using L2-norm at section 0-059.5 at some depths, from pole-dipole measurements.

The mean values from the two measurement layouts does not agree sufficiently as shown in Figure 35, i.e. an accurate estimation of the resistivity is difficult to achieve

when the values can vary between 50 and 2000 Ω m. It may however be considered that the depths are not exactly the same.

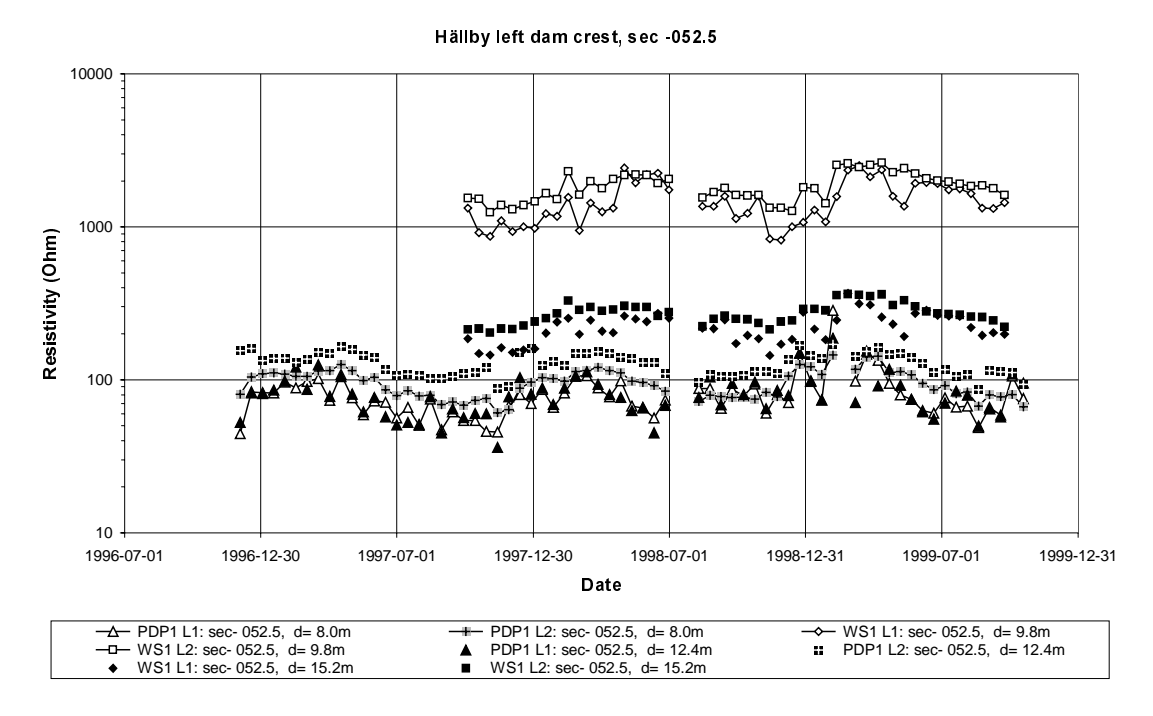


Figure 35 Evaluated resistivities at sec 0-052.5 from Wenner-Schlumberger and pole-dipole measurements.

It may also be observed that the time for the maximum values changes with depth. In section 0-052.5 lagtimes are about 3-4 months for d=9.8 and 15.2m and about 3 months for d=21.2m, either using the Wenner-Schlumberger or pole-dipole data. Those lagtimes indicate a seepage flow of about 10^{-6} m³/s, m (theoretical values between $0.5 \cdot 10^{-6}$ m³/s,m and $1.5 \cdot 10^{-6}$ m³/s,m).

Changes can also be found along the monitoring section at a certain depth as shown in Figure 36. The evaluated resistivity is lower in sec 0-038.5 and 0-024.5, while the variation seems to be almost similar in all sections. The shortest lagtime, about 3 months can be found in section 0-052.5, 0-066.5 and 0-080.5. This gives a seepage flow of about 10^{-6} m³/s,m. The lagtime in section 0-024.5 and 0-038.5 is about 4-5 months giving a seepage flow of $0.7 \cdot 10^{-6}$ m³/s,m.

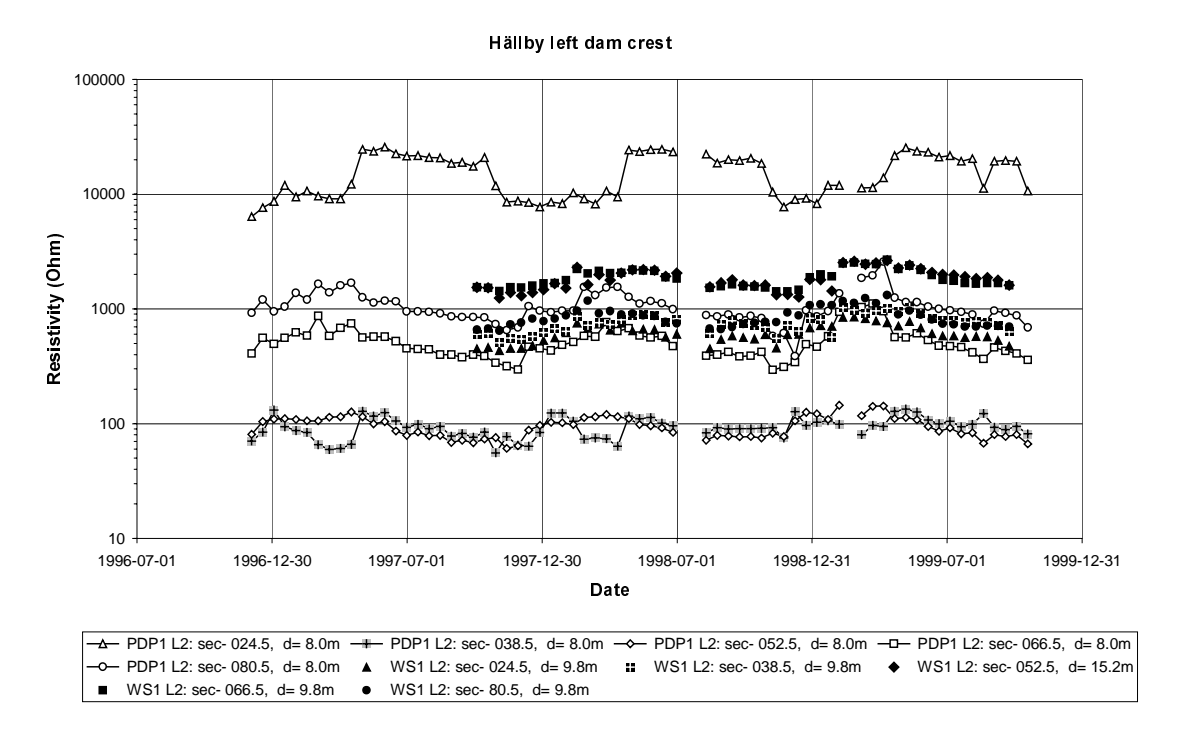


Figure 36 Evaluated resistivities (Wenner-Schlumberger and Pole-dipole) at d=8 and 9.8m in selected sections.

6.3 Right dam downstream

Data quality of the right dam downstream is even better than on the left dam crest, as concluded in sec 4.5. This is clearly showed by the temporal variation that is almost constant in some areas and depths and has a significant seasonal variation in other areas and depths, as indicated in Figure 37-40.

In section 052.5 the resistivity is almost constant in the deepest part of the section, both for Wenner-Schlumberger and pole-dipole (Figure 37 and Figure 38). This is expected because no significant resistivity variations are expected in the bedrock, where the seepage flow should be low and no material transport should occur. The limit where variations are observed is however deeper for Wenner-Schlumberger, where variations can be found down to 15 m depth.

The difference of the resistivity achieved from the used monitoring and evaluation models is smaller than those obtained from left dam crest. However, a variation between 100 and 1000 Ω m seems still to be larger than desired.

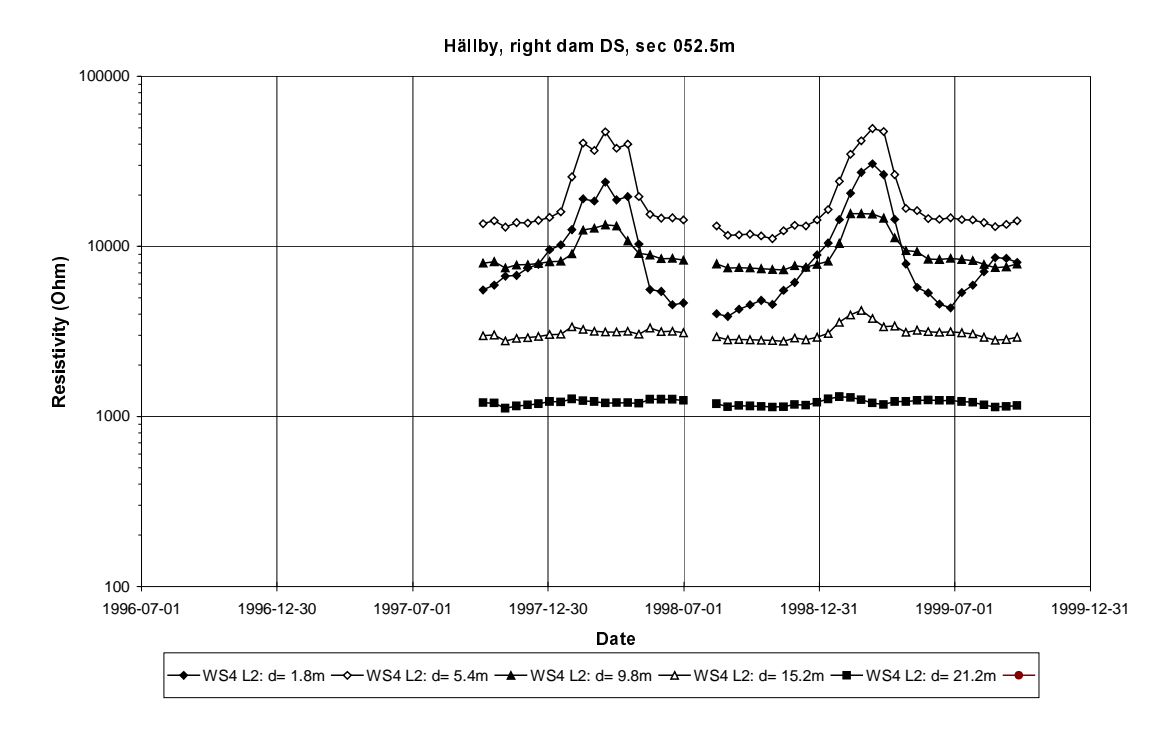


Figure 37 Evaluated resistivity using L2-norm at section 052.5 at some depths, from Wenner-Schlumberger measurements.

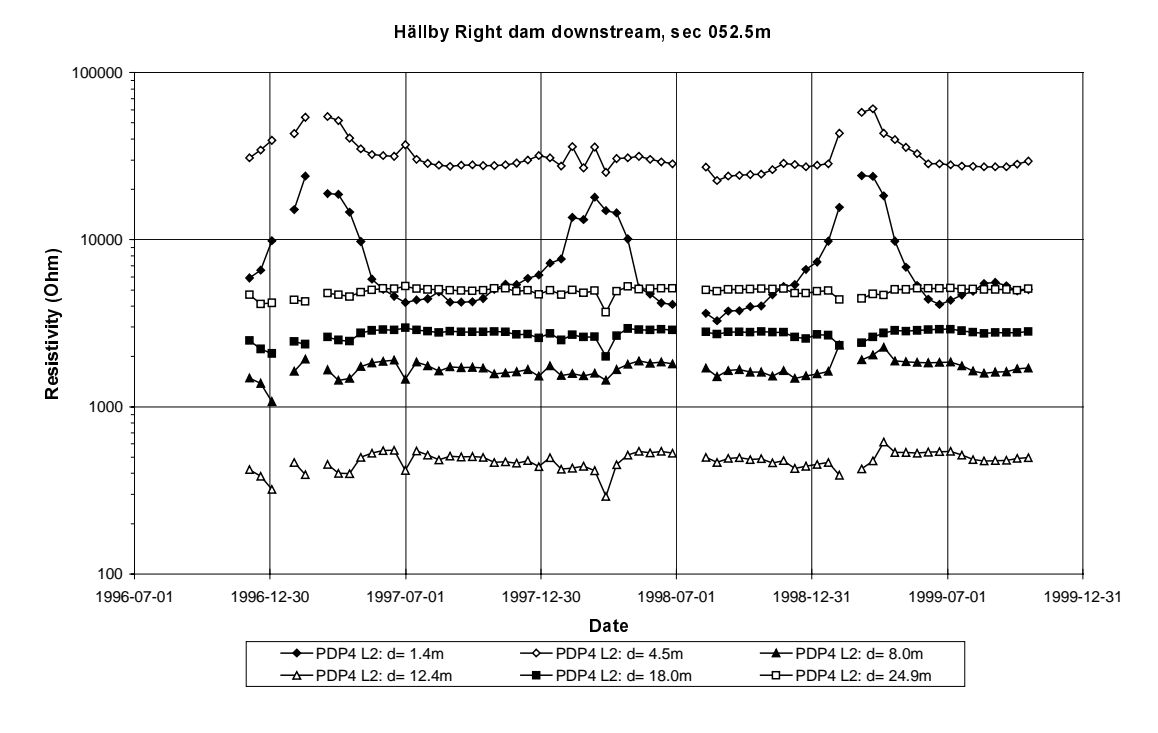


Figure 38 Evaluated resistivity using L2-norm at section 052.5 at some depths, from pole-dipole measurements.

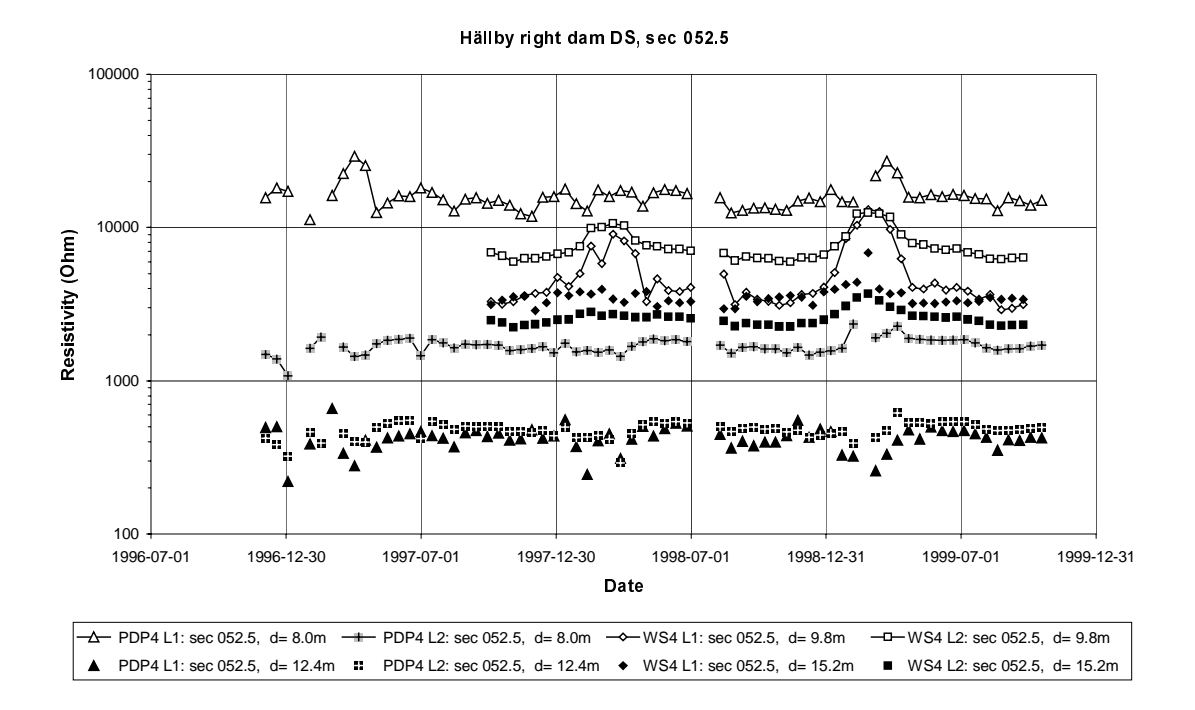


Figure 39 Evaluated resistivities (Wenner-Schlumberger and Pole-dipole using L1 or L2 norm) at d=8-9.8m and d=12.4-15.2 in section 052.5.

The seasonal variation in the deeper part of the monitoring section is probably due to seepage. The variation at d=8 and 9.8m is however larger than at left dam crest, and even larger than the variation that can be explained by temperature and TDS-variation. Other factors must then also be involved.

The resistivity variation in section 052.5 has its minimum value in October/November and its maximum in March-May, giving a lagtime of 3-5 months. The seepage flow will then be in the order of $2 \cdot 10^{-6} \text{m}^3/\text{s,m}$.

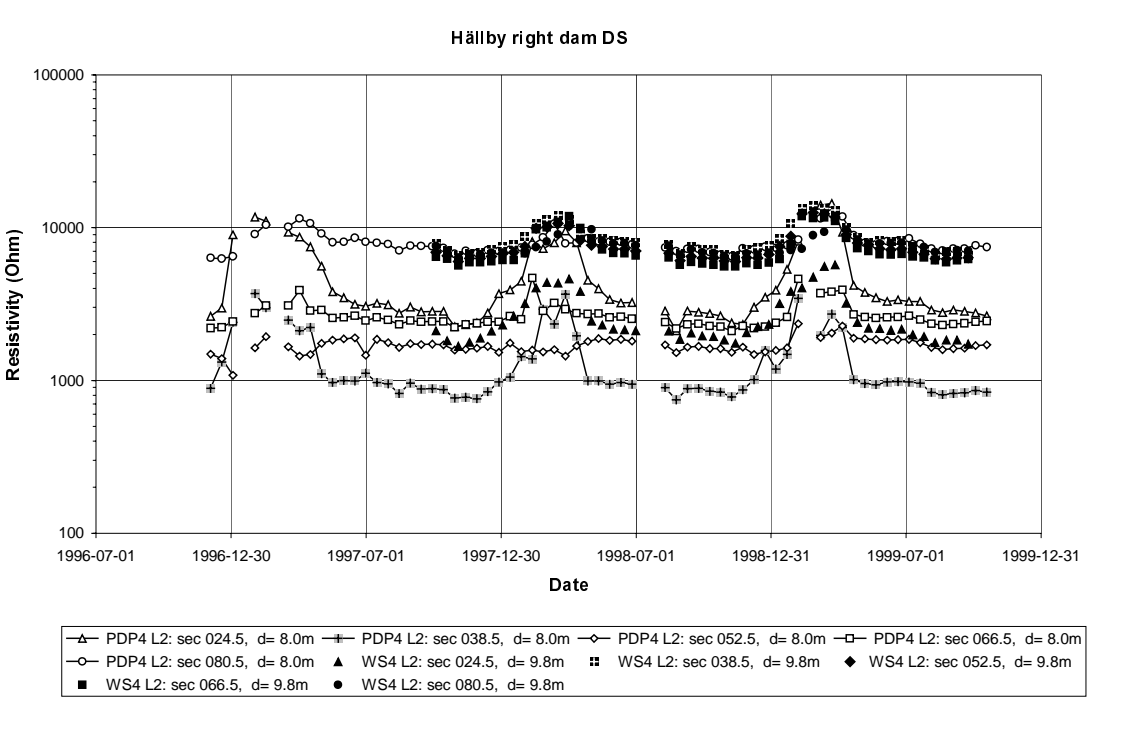


Figure 40 Evaluated resistivities (Wenner-Schlumberger and Pole-dipole) at d=8 and 9.8m in selected sections.

6.4 Discussion

The results above from some sections indicate that the resistivity variation is in the same order or less than the difference between result from the different monitoring and inversion models. Similar differences are achieved all over the dam where they generally are within a decade, see Figure 41. Some parts, however, exhibit smaller differences such as section 25, 75-90 and 100.

It may also be of interest to examine the relation between resistivity and the seasonal variation. This question is of importance for evaluation of resistivity in dams and will be further investigated. Preliminary analyses have been made on the data from the downstream section on the right dam, and the result from the Wenner-Schlumberger data is shown in Figure 42. The pole-dipole measurements show a similar result but with a larger scattering.

As a preliminary result, no significant trend can be observed for the depth level d=21m. The variation is almost constant and seems to be independent of the resistivity. A general trend for the upper parts (probably in the bedrock and below the unsaturated part) is that the variation decreases with increasing resistivity.

100000 10000 Resistivity (ohmm) 1000 ■WS4 L2 Median d= 9.8 m ■WS4 L1 Median d= 9.8 m ▲ PDP4 L2 Median d= 8.0 m PDP4 L1 Median d= 8.0 m 100 0 20 40 60 80 100 120 140 Section

Hällby right dam DS

Figure 41 Median resistivity values along Hällby right dam downstream.

Fel! Ogiltig länk.

Figure 42 Variation coefficient as a function of resistivity for right dam downstream, from Wenner-Schlumberger using L1- and L2-norm.

7 Discussion and Conclusions

Evaluated resistivities from Hällby (based on the one- or two- weeks median value) show a seasonal variation, which is interpreted to in part be a function of the seepage through the dam. This is mainly a result of the combined influence of the variation in temperature and TDS in the reservoir. These variations can be used to monitor seepage flow and locate zones of anomalous leakage. The technique is non-destructive apart from electrode installation, which is a minor intrusion on the crest of the dam.

The data measured using land-based electrodes at Hällby is associated with unsatisfactory noise levels at least for the dam crest lines. Underwater electrodes on the other hand, provide good to excellent data quality. The noise problem is to a large extent caused by high electrode contact resistance, which becomes particularly pronounced by the freezing of the ground during winter. However, it is also possible that the long leadin part of the right dam electrode cables pick up electromagnetic noise, as indicated by the higher incidence of noise for the right upstream side compared to the left upstream side.

In order to reach the data quality that is needed to extract reliable information about seepage it is essential to ascertain a better electrode grounding than is the case for the dam crest at Hällby. It has been clearly demonstrated through test measurements on electrodes installed in the Sädva dam that very good data quality can be achieved if the electrodes are installed in the upper part of the dam core, which is easily done if the height of the dam core is raised as was the case at Sädva (Johansson et al. 2000). It should be possible to develop techniques for better installation of electrodes in the upper part of the core using a drilling device as well. One option that must be considered for future work is possible ways of installing electrodes at larger depths inside the dam core, in order to make it possible to improve the resolution at depth. This will probably prove mandatory if the technique is to be employed on higher dams.

The processing and interpretation methodology of time series of resistivity data is still at a relatively early stage. Significant improvements in for example noise handling for the data are envisaged in the future. Time-lapse inversion which was used for processing the data presented here appears to be a powerful way to stabilize the inversion process (Loke 1999b), and the results presented here are more consistent than in previous processing version of the first years of data (Johansson and Dahlin 1998; Johansson and Dahlin 1999). However, a more systematic assessment of the potential and limitations need to be carried out, against field data as well as numerical models. For example, it should be noticed that it has at this stage not been possible to experiment with different parameter settings for the inversion, such as smoothness factors and whether L1-norm or L2-norm is preferable in different situations, so the results presented here are most likely not optimized.

The data sets behind the inverted sections presented here are relatively small due to the limited number of electrodes in each layout line. This is a serious limitation since the data density is of major importance for the resolution and reliability of the inverted

model sections (Dahlin and Loke 1998). However, there is a limit to how many different combinations can be made for each array type, and one way of getting around this may be to combine different electrode arrays in the same inversion round, such as Wenner-Schlumberger and pole-dipole. For the pole-dipole data there is in fact a higher data density recorded since the end of February 1999, which was not used here in order to keep the same data density throughout the analyzed period.

Seepage flow can be evaluated from the resistivity data using methods similar to those employed for seepage evaluation from temperature data. Seepage flow is generally in the order of 10⁻⁶m³/s,m², but the evaluation methods must be improved.

SP-data recorded at Hällby using stainless steel electrodes are stable, and where present the seasonal variation is also stable and repeatable. The appearance of the data indicates that they are contaminated with an electrode polarisation noise. This is also borne out by the observation that there is only a seasonal variation in the three land-based profiles. As there is no, or very little, seasonal variation in the offshore data one can only conclude that the major part of the seasonal variation observed is caused by polarisation effects, which change as the local environmental conditions do. The regular nature of the seasonal variation argues that it could be possible to quantify the variation and remove it from data. To achieve this, longer historical records than are available now are probably necessary.

Subtracting the mean SP-profile from each recording should remove some of the static electrode polarisation noise. On the offshore profiles this technique is quite effective, indicating that the electrode environment is stable. Some weak changes in residual SP-values appear in these data, possibly indicating seepage variation. The technique does not really work with the land-based profiles where changes in local electrode environment produce the major part of the time-variation of SP. No reliable changes in residual SP, apart from the seasonal variation could be identified.

It is obvious that the use of stainless steel electrodes for SP measurements introduces several complicating factors in the interpretation. Processing of the data can to a certain extent remove polarisation effects, but the results will never be as good as if non-polarising electrodes were used. It seems reasonable, though, to continue to refine the techniques for processing data of the type acquired at Hällby, since installation of special SP electrodes is not always feasible.

Overall results and experience do not yet allow an installation of an automatic seepage monitoring system. However, both monitoring and evaluation methods can be improved. The method may then be an alternative for seepage monitoring in existing dams, without seepage monitoring systems, or where conventional seepage monitoring is complicated.

In conclusion, the seasonal resistivity variation can be significant in embankment dams and cannot be assumed to be constant. If resistivity measurement is performed in a dam

on a single occasion the result must be interpreted carefully because the result is incomplete without the time variation and may even be misleading.

8 Acknowledgements

This work, as well as previous work, has been performed within a several projects mainly funded by the research company Elforsk AB. The dam owner, Birka Energi AB, has given additional funding and valuable support, especially the personnel at the dam site with installation and occasional maintenance of the monitoring system.

9 References

- [1] Dahlin, T. (1993) On the Automation of 2D Resistivity Surveying for Engineering and Environmental Applications, Ph.D.Thesis, ISRN LUTVDG/TVDG--1007--SE, ISBN 91-628-1032-4, Lund University, 187p.
- [2] Dahlin, T. (1996) 2D resistivity surveying for environmental and engineering applications, First Break, vol 14, no 7, p 275-283.
- [3] Johansson, S. (1991), Localization and quantification of water leakage in ageing embankment dams by regular temperature measurements. Q65, R54, ICOLD 17th Congress in Vienna.
- [4] Johansson, S. (1997), Seepage Monitoring in Embankment Dams, Doctoral Thesis, TRITA-AMI PHD 1014, ISBN 91-7170-792-1, Royal Institute of Technology, Stockholm.
- [5] Johansson, S. and Dahlin, T. (1996) Seepage monitoring in an earth embankment dam by repeated resistivity measurements, European Journal of Engineering and Environmental Geophysics, vol 1, no 3, p 229-247.
- [6] Johansson, S. and Dahlin, T. (1998) Seepage monitoring in Hällby embankment dam by continuous resistivity measurements, 8th Congress of the International Association for Engineering Geology and the Environment, Vancouver, p95-102, ISBN 90 5410 991 2
- [7] Johansson, S. and Dahlin, T. (1999) Övervakning av läckage i fyllningsdammar genom resistivitetsmätning, Report 99:8, Elforsk, Stockholm, 55p.
- [8] Johansson, S., Dahlin, T., Farhadrioushan, M. and Friborg, J. (2000) Experience from Initial Resistivity, SP, Strain and Temperature Measurements at Sädva, Report 00:14, Elforsk, Stockholm, 22p.
- [9] Loke, M.H. and Barker, R.D. (1996) Rapid least-squares inversion of apparent resistivity pseudosections by a quasi-Newton method, Geophysical Prospecting, vol 44, no 1, p 131-152.
- [10] Loke, M.H. (1999a) Res2dinv ver 3.4 for Windows 3.1, 95 and NT. Rapid 2-D resistivity & IP inversion using the least squares method, software manual, http://www.abem.se, 81p.
- [11] Loke, M.H. (1999b) Time-lapse resistivity imaging inversion, Procs. 5th Meeting of the European Association for Environmental and Engineering Geophysics, 5-9 September 1999, Budapest, Em1, 2p.
- [12] Parasnis, D.S. (1986) Principles of applied geophysics, 4:th ed, Chapman and Hall, London, 402p.
- [13] Sill, W.R. (1983) Self-potential modelling from primary flows, Geophysics, v. 48, no 1, p76-86.
- [14] Triumf, C.-A. and Thunehed, H. (1996) Two years of Self-Potential measurements on a large dam in northern Sweden. *Repair and Upgrading of Dams, Proceedings, KTH,* Stockholm, p307-315.
- [15] Ward, S.H. (1990) Resistivity and Induced Polarization Methods, in Investigations in Geophysics no. 5: Geotechnical and Environmental Geophysics, vol I, ed. S. Ward, Society of Exploration Geophysicists, Tulsa, p 147-189.



SVENSKA ELFÖRETAGENS FORSKNINGS- OCH UTVECKLINGS - ELFORSK - AB Elforsk AB, 101 53 Stockholm. Besöksadress: Olof Palmes Gata 31 Telefon: 08-677 25 30. Telefax: 08-677 25 35. E-post: <u>info@elforsk.se</u> www.elforsk.se.